Common Land Model (CLM)

(Technical Documentation and User's Guide)

Yongjiu Dai, Xubin Zeng, and Robert E. Dickinson

and

COAUTHORS

(2001)

CONTENTS

List of Tables

List of Figures

Mathematical Symbols

$\bar{\alpha}_{\Lambda,\mu}$ Weighted surface albedo [visible (beam, diffuse), near-infrared (beam, diffuse)] over grid
$\bar{\alpha}_{\Lambda,\mu(c)}$ Effective albedo over vegetation with snow
$\bar{\alpha}_{\Lambda,\mu(g)}$ Effective albedo over bare soil covered snow
$\alpha_{\Lambda,\mu(f)}$ Single leaf albedo
$\alpha_{\Lambda,\mu(g)}$ Bare soil albedo
α_{sat} Saturated soil albedo
α Quantum efficiency (μmol CO_2 per μmol photon)
$\delta_{k'k}$ Kronecker delta
ε_{34} Quantum efficiency at 25 ^{o}C (μmol CO_2 / μmol photon)
ε_g Emissivity of the ground
ε_v Emissivity of the vegetation
ϕ_{sha} Photosynthetically active radiation absorbed by shaded leaves (W m^{-2})
ϕ_{sun} Photosynthetically active radiation absorbed by sunlit leaves (W m^{-2})
λ_k Thermal conductivity of constituent k, k = a (air), d (dry soil), i (ice), w (liquid), sat (saturated soil) (W $m^{-1}K^{-1}$)
μ Cosine of solar zenith angle (-)
ν Kinematics viscosity of air ($m^{-2}s$)
θ Volumetric content of liquid water (m^3m^{-3})
θ_a Air potential temperature at reference height (K)
θ_k Partial volume of constituent k, k = d (dry soil), i (ice), l (liquid) (m^3m^{-3}),
θ_s Surface air potential temperature at height z_{0h}+d (K)
θ_{sat} Porosity
θ_* Turbulence temperature scale (K)
θ_{*v} Turbulence temperature scale (K)
ρ_k Intrinsic density of constituent k, k = a (air), d (dry soil), i (ice), l (water) (kg m^{-3})
ρ_s Snow density (kg m^{-3})
σ Stefan-Boltzmann constant (W $m^{-2}K^{-4}$)
σ_f Fraction of vegetation excluding the part by snow buried

ς Turbulent stability parameter
τ_x Zonal momentum flux (kg $m^{-1}s^{-2}$)
τ_y Zonal momentum flux (kg $m^{-1}s^{-2}$)
τ_{snow} Non-dimensional age of snow
ω Weighting coefficient in time domain
$\omega\beta_0$ Upward scattered fraction for direct beam
ω_v Leaf-scattering coefficient (single scattering albedo) for PAR (-)
ψ_{sat} Saturated soil matrix potential (mm)
ψ Soil matrix potential (mm)

Δz_j Soil and snow layer thickness (j = snl+1, ...,-1, 0, ..., msl) (m)
Γ_* CO2 compensation point (pa)

a Coefficient for thermal roughness
a_j Coefficient of the tridiagonal matrix
a_{kc} Temperature sensitivity parameter for K_{c25}
a_{ko} Temperature sensitivity parameter for K_{o25}
$a_{v\,max}$ Temperature sensitivity parameter for $V_{max\,25}$
b Minimum leaf conductance (μmol $m^{-2}s^{-1}$)
b_j Coefficient of the tridiagonal matrix
c_{34} Photosynthetic pathway for c_3 and c_4 plants
c_a A tunable parameter
c_a Atmospheric CO_2 concentration (pa)
c_i Internal leaf CO_2 concentration c_i (pa)
c_j Coefficient of triadiagonal matrix
c_k Specific heat of constituent k, k = d (dry soil), i (ice). l (liquid water) (J $kg^{-1}K^{-1}$)
c_p Specific heat for dry air (J $kg^{-1}K^{-1}$)
c_s CO_2 concentration at the leaf surface
d Canopy zero plane displacement (m)
d_{sn} Total snow depth (m)
e_a Vapor pressure of canopy air (pa)
e_i Vapor pressure inside leaf (pa)
e_s Vapor pressure at the leaf surface e_s (pa)
e'_a Vapor pressure of canopy air with lower limit imposed (pa)
f Scaling parameter controlling the rate of $K_{sat\,max}$ decline (m^{-1})
$f_{root,j*}$ Effective root fraction
f_{root} Fraction of root
f_{sha} Shaded fraction of canopy

f_{sun} Sunlit fraction of canopy

g Gravity constant (m s^{-2})

h_k Enthalpy of constituent k, k = d (dry soil), i (ice), l (liquid water), v (vapor) (J kg^{-1})

h_r Relative humidity of ground surface air

k von Kárman constant

k_b PAR extinction coefficient for direct beam solar radiation (-)

k_d PAR extinction coefficient for diffuse solar radiation (-)

m Slope of stomatal conductance-photosynthesis relationship (-)

msl Number of soil layers

o_i Atmospheric O_2 concentration (pa)

p_l Lowest model level air pressure (pa)

p_s Surface air pressure (pa)

q Water flow between two neighbor layers, positive (downward) (kg $m^{-2}s^{-1}$)

q_* Humidity scale

q_0 Water flux at ground surface, positive (downward)

q_a Lowest model level water-vapor specific humidity (kg kg^{-1})

q_{af} Air specific humidity within canopy space (kg kg^{-1})

q_g Air specific humidity of ground surface air (kg kg^{-1})

q_j Water flux through the interface of j and j+1 layers

$q_{j(ice)}$ Rate of ice mass onto the interface of j and j+1 layers (mm s^{-1})

q_s Surface air humidity a height $z_{0q} + d$ (kg kg^{-1})

q_{sat} Saturated specific humidity

r_{ah} Aerodynamic resistance for sensible heat (s m^{-1})

r_{am} Aerodynamic resistance for momentum (s m^{-1})

r_{aq} Aerodynamic resistance for water vapor (s m^{-1})

r_b Leaf boundary resistance (s m^{-1}, s m^2 μmol^{-1})

r_d Aerodynamic resistance between ground and canopy air

r_j Coefficient of the tridiagonal matrix

r_s Leaf stomatal resistance (s m^{-1}, s m^2 μmol^{-1})

snl Number of snow layers (negative)

s_r Irreducible water in snow

u_* The surface friction velocity

u_s Lowest model level west to east wind component (m s^{-1})

v_s Lowest model level south to north wind component (m s^{-1})

w_* Convective velocity scale

w_{dew} Canopy interception water store (mm)

$w_{d\,max}$ Maximum water the canopy can hold (mm)

w_{ice} Mass of ice of soil or snow layers (kg m^{-2})

w_c RuBP carboxylase (Rubisco) limited rate of carboxylation (μmol CO_2 m^{-2} s^{-1})

w_e Export limited rate of carboxylation for C_3 plants and the PEP carboxylase limited rate of carboxylation for C_4 plants (μmol CO_2 m^{-2} s^{-1})

w_j Maximum rate of carboxylation allowed by the capacity to regenerate RuBP (i.e., the light limited rate) (μmol CO_2 m^{-2} s^{-1})

w_{liq} Mass of water of soil or snow layers (kg m^{-2})

z_{0h} Thermal roughness

z_{0m} Aerodynamic roughness length (m)

z_{0v} Canopy roughness length (m)

$z_{h,j}$ Depth at the interface of soil / snow layer j and j+1 (m)

z_i Convective boundary layer height

z_j Depth of soil (or snow) layer j at the node depth (m)

z_r Height of the lowest model level (or called reference height) (m)

A Leaf photosynthesis (μmol CO_2 $m^{-2}s^{-1}$)

B Exponent B defined in Clapp & Hornberger

C_f Coefficient of transfer between foliage and air in the foliage

C_R Total fraction of the natural compaction rate

C_{soilc} Transfer coefficient between the canopy air and underlying ground

D_d Direct throughfall the gaps of leaves (mm s^{-1})

D_f Characteristic dimension of leaves in wind direction

D_r Outflow of water stored on leaves and stem (mm s^{-1})

E Water flux (kg $m^{-2}s^{-1}$)

E_a Evapotranspiration to atmosphere (kg $m^{-2}s^{-1}$)

E_c Sum of transpiration and evaporation from wet foliage (kg $m^{-2}s^{-1}$)

E_f Potential evaporation (kg $m^{-2}s^{-1}$)

E_g Evaporation from ground (kg $m^{-2}s^{-1}$)

$E_{g(e)}$ Evaporation from ground (or condense)

$E_{g(s)}$ Rate of sublimation (or frost) (kg $m^{-2}s^{-1}$)

E_{tr} Transpiration (kg $m^{-2}s^{-1}$)

$E_{tr\,max}$ Maximum transpiration rate (kg $m^{-2}s^{-1}$)

E_w Evaporation for wet foliage (kg $m^{-2}s^{-1}$)

$F_{\Lambda,\mu(c)}$ Fraction of solar radiation absorbed by canopy

F_{AGE} A transformed snow age

F_j Heat flux across the interface between layer j and j+1

F_{sn} Fraction of vegetation buried (covered) by snow:

F_{veg} Fraction of vegetation cover

G Projection of leaves in direction of incoming radiation flux (-)
H Sensible heat flux (W m^{-2})
H_a Sensible heat flux to atmosphere (W m^{-2})
H_c Sensible heat flux from foliage to canopy air (W m^{-2})
H_g Sensible heat flux from ground to canopy air (W m^{-2})
I_b Direct beam solar radiation (visible) absorbed by the canopy (W m^{-2})
I_d Diffuse solar radiation (visible) absorbed by the canopy (W m^{-2})
K Hydraulic conductivity (mm s^{-1})
K_c Michaelis-Menten constants (poa) for CO_2
K_{c25} CO_2 michaelis-menten constant at 25°C (pa)
K_e Function of the degree of saturation
K_o Michaelis-Menten constants (pa) for O_2
K_{o25} O_2 michaelis-menten constant at 25°C (pa)
K_{sat} Saturated hydraulic conductivity (mm s^{-1})
$K_{sat\,max}$ Saturated hydraulic conductivity (mm s^{-1})
L Monin-Obukhov length
$L_a^{\downarrow}$ Incident atmospheric long wave radiation (W m^{-2})
L_{AI} Leaf area index (m^2 m^{-2})
L_d Dry fraction of foliage surface
LE Latent heat flux (W m^{-2})
L_f Latent heat of fusion for ice (J kg^{-1})
$L_g^{\uparrow}$ Outgoing longwave radiation from surface (W m^{-2})
$L_{n,c}$ Net longwave radiation absorbed by canopy (W m^{-2})
$L_{n,g}$ Net longwave absorbed by ground (W m^{-2})
L_s Latent heat of sublimation (J kg^{-1})
L_{sha} Shaded leaf area index
L_{sun} Sunlit leaf area index
L_v Latent heat of evaporation for water (J kg^{-1})
$\tilde{L}_w$ Wetted fraction of the canopy
L_{AI} Leaf area index (m^2 m^{-2})
L_{SAI} Stem plus leaf area index (m^2 m^{-2})
$M_{k'k}$ Phase change from phase k' to phase k (kg $m^{-3}s^{-1}$)
M_{il} Rate of phase change (ice to liquid) (kg $m^{-3}s^{-1}$)
N Foliage nitrogen (%)
N_{max} Maximum foliage nitrogen (%)
P Precipitation rate (mm s^{-1})
P_{AR} Photosynthesis active radiation absorbed per unit L_{AI} (W m^{-2})
P_r Rate of precipitation falling as rain (mm s^{-1})

P_s Rate of precipitation falling as snow (mm s^{-1})
R Gas constant for dry air (J $kg^{-1}K^{-1}$)
$R_{n,c}$ Net radiation absorbed by canopy (W m^{-2})
$R_{n,g}$ Net radiation absorbed by ground (W m^{-2})
R_s Surface runoff (mm s^{-1})
R_g Drainage at the bottom of soil layers (mm s^{-1})
R_w Gas constant for water vapor (J $kg^{-1}K^{-1}$)
$S^{\downarrow}_{\Lambda,\mu}$ Component of the incident solar radiation visible (beam and diffuse), near-infrared (beam and diffuse) (W m^{-2})
S_{AI} Stem area index (m^2 m^{-2})
S_{cv} Fraction of soil covered by snow
S_k Source or sink term
S_n Net solar absorbed by surface (canopy+ground) (W m^{-2})
$S_{n,c}$ Net solar absorbed by canopy (W m^{-2})
$S_{n,g}$ Net solar absorbed by ground (W m^{-2})
$S^{\downarrow}_{\Lambda,\mu}$ Downward direct beam visible solar radiation (W m^{-2})
T_a Lowest model level air temperature (K)
T_{af} Air temperature within canopy space (K)
T_c Leaf temperature (K)
T_f Freezing temperature (K)
T_j Temperature at the j^{th} node of soil or snow (K)
T_{min} Minimum temperature at which plants photosynthesize (ºC)
T_v Leaf temperature (ºC)
U_{af} Magnitude of wind within the foliage layer (m s^{-1})
U_k Mass flux (kg $m^{-2}s^{-1}$),
V_a Wind at reference height (m s^{-1})
V_{max} Maximum rate of carboxylation (µmol CO_2 m^{-2} s^{-1})
$V_{max\,25}$ Maximum rate of carboxylation at 25ºC (µmol CO_2 m^{-2} s^{-1})

Subscripts
a Air
b Direct solar beam
c Canopy
d Dry soil constituent, diffusion solar beam
f Single leaf
g Ground
i Ice
ir near-infrared solar
k Index of constituent

j	Node index
l	Liquid water
s	Snow
sat	Saturated state
sha	Shaded leaves
sun	Sunlit leaves
v	Vapor, visible solar
μ	Direct, diffuse
Λ	Visible, near-infrared

Superscripts

n	index of time step

1. Introduction

The Common Land Model (CLM) is a project that is multi-disciplinary and multi-institutional and whose intent is to develop a state of the art land surface model for use in climate studies. It requires broader expertise than found in any one research group or institution. This report documents the initial prototype version of this model.

The CLM derives from the premise that if a land model could be constructed from components used in most land models and in a way acceptable to the community, then individual groups that are interested in land modeling but lacking the necessary resources or expertise, could focus on the new aspects without excessive repetition of past efforts. Furthermore, all the users of such a CLM, in the spirit of 'open source' code development, could then share the improvements and refinements provided by individual groups.

The CLM was originally proposed to provide a framework for a truly community-developed land component of the NCAR CSM at a workshop of the NCAR CSM Land Working Group in February 1996. An opportunity to advance this concept was provided by a visit to the US of Yongjiu Dai from the Beijing / China (Institute of Atmospheric Physics, Chinese Academy of Sciences), hosted by Xubin Zeng (University of Arizona) and supported with funding from a NASA /EOS Interdisciplinary Science Project. Initial specifications of the software to be developed were given by Robert Dickinson, who suggested that the goal of a truly common land model was unlikely to be achieved within existing institutions but that it would be useful to provide a prototype that could demonstrate at least some groups were motivated and capable of joining forces to produce a shared model.

One important starting point was Gordon Bonan's (NCAR) well-documented LSM land code, currently in use as part of the NCAR CSM climate model. Dai had already demonstrated extensive familiarity with the IAP LSM (version 1994, IAP94) code (his PhD), as well as the BATS code that had been the starting point of his IAP94 code. Thus, it was decided that Dai, with sufficient help, could effectively implement a state of the art model that combined best features of the LSM, BATS, and IAP94 codes. Hence, early in 1998, Dai, Dickinson, and Zeng reviewed the content of these codes and developed initial software specifications. It was also seen as highly desirable that the resulting model not only be targeted as a next generation model for the land component of the NCAR CSM but also as a candidate for next generation used by other US groups requiring extensive revisions of their current land surface models.

Various conversations indicated interest in potential application for the needs of the GSFC DAO modeling structure, which was initially implementing Koster's MOSAIC model, and COLA scientists tasked with revision of their SSiB model. Ties to groups concerned with carbon cycle and ecological modeling were also desired. Initial specifications of the design were reviewed and commented on by an ad hoc CLM scientific steering committee, chaired by CSM LWG chairs (Dickinson and Bonan), and with initial membership besides Dai and Zeng, was Paul Dirmeyer (Center for Ocean-

Land-Atmosphere Studies), Jay Famiglietti (University of Texas-Austin), Jon Foley (University of Wisconsin), and Paul Houser (GSFC). Dirmeyer and Houser provided especially substantive guidance as to how the code could be improved in ways that would better meet their institutional requirements. Zeng took on the role of coordinating this community input and in working with Dai to oversee its implementation. The improved software implementation plan consequently developed was discussed at the June 1998 annual CSM Workshop and finalized by Dai and Zeng. Dai subsequently constructed an initial code that was scrutinized for 3 days in March 1999 by an outside review committee consisting of Bosilovich, (GSFC), Dirmeyer, and Houser.

At this point an extensive period of "beta-testing" of this code was initiated and lasted for more than a year. At the University of Arizona, Zong-Liang Yang joined Dai, Dickinson, and Zeng in this effort, whereas the participation of Bonan at NCAR was strengthened by Keith Oleson. COLA provided Schlosser to join Dirmeyer's participation, and GSFC/DAO's participation continued through Houser and Bosilovich. Denning and Baker of Colorado State University also joined this model testing as part of their effort to establish a next generation SiB model. Initial results from this testing were presented during the CLM workshop at COLA in November 1999. Site data used for validation included all the PILPS sites and others, in particular that of Cabauw, Valdai, FIFE, ARME, ABRACOS, HAPEX, BOREAS, and WLEF, the regional data of the Red-Arkansas basin, and the Global Soil Wetness Project (GSWP) data. Validation of applications requires actually testing in those applications. Initial such applications have included use in the multi-agency Land Data Assimilation project (LDA), and coupling to CCM3.

The code design specification has emphasized various aspects of modularity. Three logically separate elements were defined: a) the core single-point model process code, b) the boundary condition data, and c) a driver that interfaces the land model to the atmosphere (including the scaling procedures within a climate model required to interface atmospheric model grid-square inputs to land single-point processes). Such separation allows the best science to be used for each of these elements, and in particular, to insure that a) the core model can be tested with single-point field data, b) the latest boundary condition data sets as derived from NASA satellite data can be incorporated when available, and c) the latest concepts as to scaling procedures can be adopted. This report primarily documents the point model treatment. Some advances in data sets and scaling are also described here, but these questions require much further effort. The code has been developed in FORTRAN, currently FORTRAN 90, to be most compatible with existing codes and scientist's programming expertise. Houser developed an interface (coupler) routine to isolate the land code from the requirements of needing model data structures.

Some aspects of the CLM are relatively complex as required to be general enough to satisfy a wide variety of anticipated applications. Managing such complexity is not easy. However, we anticipate that good documentation and the open scrutiny of many scientists will eliminate any serious errors. More limited applications may require more simplified treatments. For example, the multi-layer soil and snow structure is needed to provide

accurate simulation over a wide variety of time scales, and hence to be useful for such disparate applications as model data assimilation of surface properties, or correctly determining soil temperatures beneath snow for matching measurements of soil respiration. The suggestion has been made that a variety of simpler models also be provided. In particular, a much simpler slab treatment could be used for the limited requirement of providing sensible and latent fluxes to the atmosphere. However, our limited resources have not yet permitted taking on such an effort. Furthermore, there is considerable interest in further improvements, and likely increased complexity, for many aspects of the current code. These include the parameterization of runoff, and better integration into models of vegetation dynamics and soil biogeochemistry.

2. Model Structure

This section will describe the model data, the prognostic variables and interface requirement for off-line run and coupling to GCM.

2.1 Horizontal and vertical representations

Every surface grid cell can be subdivided into any number of tiles, and each tile contains a single land cover type. By default, each grid box is divided into up to five tiles with a fraction: dominant vegetation type with a cell fraction, secondary vegetation with a cell fraction, bare soil with a cell fraction, wetland with a cell fraction, and inland water with a cell fraction (Figure 2.1).

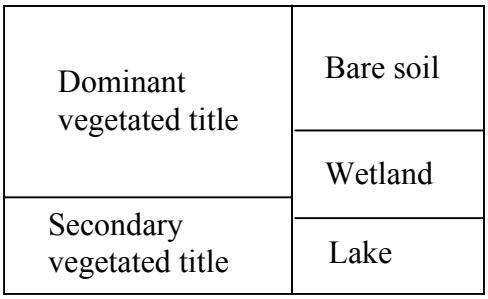

Figure 2.1. Schematic of tile subdivided for a grid box.

Energy and water balance calculations are performed over each tile at every time step, and each tile maintains its own prognostic variables. The tiles in a grid square respond to the mean conditions in the overlying atmospheric grid box, and this grid box, in turn, responds to the areally-weighted fluxes of heat and moisture from the tiles. The tiles within a grid square do not interact with each other directly.

CLM has one vegetation layer, 10 unevenly spaced vertical soil layers, and up to 5 snow layers (depending on the total snow depth). The details can be found in section 3.1 and the structure is shown in Figure 2.2.

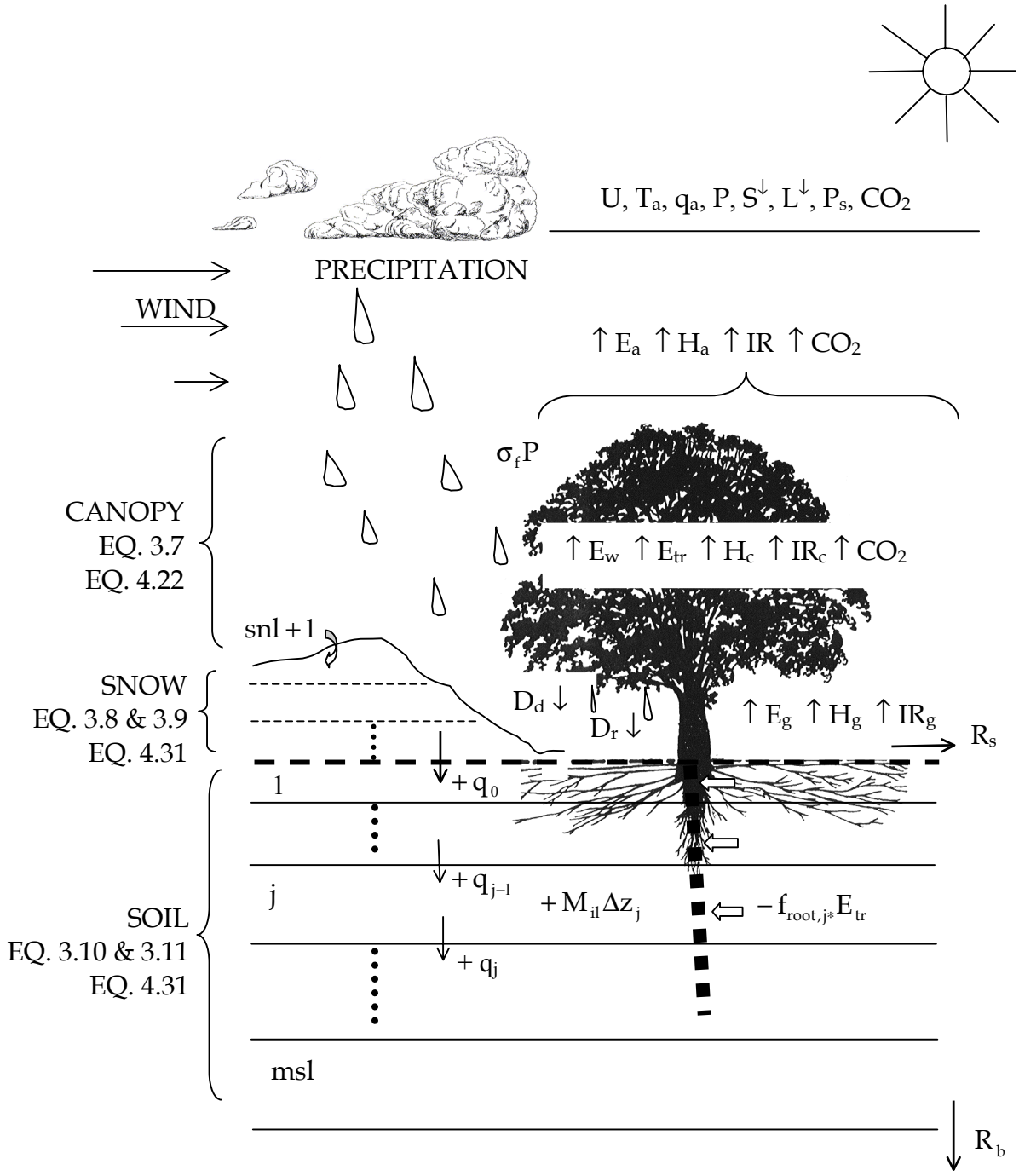

Figure 2.2. Structure of the CLM model. CLM has one vegetation layer, ten soil layers and up to 5 snow layers depending on the snow depth.

(Expect to be filled or re-shaped, especially, expect the contributions from the guys who have talent sense on such kind of figuring – BONAN, HOUSER and DIRMEYER…)

2.2 *Surface data*

Required surface data for each land grid or in site are listed in Table 1.

Table 2.1. Required surface data

Data	Purposes
Latitude and longitude at center of grid	For calculation of the solar zenith angle
Soil color type of grid cell (or sub-grid)	For calculation of the saturated and dry soil albedo in two wavelength regions
Percentages of sand and clay of soil of grid cell (or sub-grid) with vertical profile	For calculation of the soil thermal and hydrological properties
Land cover type of each sub-grid	Define the plant types, which differ in ecological characteristics and radiative transfer. IGBP land cover classification (see Table A3) is taken by default, other definition of classification can be controlled by the user.
Fraction of each sub-grid covered with land cover type	Fluxes up-scaling

The surface data need to be prepared for each tile.

2.3 *Soil Physical Properties*

(a) Parameters related to the content of sand and clay of soil
The soil thermal and hydraulic parameters ($\rho_d c_d$, λ_d, θ_{sat}, ψ_{sat}, K_{sat} and B) are produced by soil texture. Soil textural classes are determined uniquely by a combination of three variables, the percent of total masses of clay and silt and sand of soil. The soil thermal and hydraulic properties are given in Bonan (1996) as follows:

The specific heat capacity of soil solid:

$$\rho_d c_d = \frac{2.128\%\,\text{sand} + 2.385\%\,\text{clay}}{\%\,\text{sand} + \%\,\text{clay}} \times 10^6, \ (\text{J m}^{-3}\text{K}^{-1}) \tag{2.1}$$

The thermal conductivity of soil solids:

$$\lambda_d = \frac{8.80\%\,\text{sand} + 2.92\%\,\text{clay}}{\%\,\text{sand} + \%\,\text{clay}}, \ (\text{W m}^{-1}\text{K}^{-1}) \tag{2.2}$$

The porosity:

$$1 - \theta_d = \theta_{sat} = 0.489 - 0.00126\ (\%\,\text{sand}), \ (\text{m}^3\,\text{m}^{-3}) \tag{2.3}$$

The saturated matrix potential:

$$\psi_{sat} = -10 \times 10^{1.88 - 0.013(\%\text{sand})}, \ (\text{mm}) \tag{2.4}$$

The saturated hydraulic conductivity:

$$K_{sat\,max} = 0.0070556 \times 10^{-0.884 + 0.0153(\%\text{sand})}, \ (\text{mm s}^{-1}) \tag{2.5}$$

The exponent B defined in Clapp & Hornberger (1978):

$$B = 2.91 + 0.159\ (\%\,\text{clay}) \tag{2.6}$$

(b) Parameters related to soil colors
Soil albedo is taken as a function of soil wetness and the albedo of saturated and dry soil (section 6.3). The values of albedo for light soil to dark soil at saturation and dry soil conditions are listed in Table 2.2, which are adopted from BATS (Dickinson et al. 1993).

Table 2.2. Saturated and Dry Soil Albedo (Color from light to dark)

	1	2	3	4	5	6	7	8	9*
a) Saturated Soil Albedo									
< 0.7 μm	0.12	0.11	0.10	0.09	0.08	0.07	0.06	0.05	0.15
≥ 0.7 μm	0.24	0.22	0.20	0.18	0.16	0.14	0.12	0.10	0.31
b) Dry Soil Albedo									
< 0.7 μm	0.23	0.22	0.20	0.18	0.16	0.14	0.12	0.10	0.27
≥ 0.7 μm	0.46	0.44	0.40	0.36	0.32	0.28	0.24	0.20	0.55

* a special class created by Bonan (1996) for better matching ERBE clear-sky abledos for desert and semi-desert located in North Africa and Arabian Pesinsula.

2.4 *Vegetation Properties*

(a) Time-invariant parameters
Each vegetation type is assigned a set of time-invariant parameters, which are treated as constants. These include:

(i) Optical properties

$\alpha_{v,\mu(f)}$ Vegetation albedo for wavelengths < 0.7 μm

$\alpha_{ir,\mu(f)}$ Vegetation albedo for wavelengths > 0.7 μm

with the same value for direct beam (μ=b) and diffusion (μ=d).

(ii) Morphological properties

z_{0v} Canopy roughness length (m)

d Canopy zero plane displacement (m)

$D_f^{-1/2}$ Inverse square root of leaf dimension ($m^{-1/2}$)

$f_{root}[z]$ Root fraction from the surface to depth z:

$$f_{root}[z] = 1 - 0.5\,[\exp(-az) + \exp(-bz)]$$

where coefficients *a* and *b* are dependent upon vegetation types, and are given in Table 2.3.

Table 2.3: Vegetation / Land Cover Time-invariant Parameters

IGBP TYPE	$\alpha_{v,\mu(f)}$	$\alpha_{ir,\mu(f)}$	z_{0v}	d	$D_f^{-1/2}$	a	b	d_r

1	0.05	0.23	1.0	9.0	5.0	6.706	2.175	1.8
2	0.04	0.20	2.0	18.0	5.0	7.344	1.303	3.0
3	0.05	0.23	1.0	9.0	5.0	7.066	1.953	2.0
4	0.08	0.27	0.8	1.0	5.0	5.990	1.955	2.0
5	0.06	0.24	0.8	0.5	5.0	4.453	1.631	2.4
6	0.07	0.26	0.1	0.0	5.0	6.326	1.567	2.5
7	0.14	0.32	0.09	0.0	5.0	7.718	1.262	3.1
8	0.07	0.25	0.8	1.0	5.0	7.604	2.300	1.7
9	0.08	0.30	0.1	0.0	5.0	8.235	1.627	2.4
10	0.10	0.30	0.02	0.0	5.0	10.74	2.608	1.5
11	0.06	0.18	0.03	0.0	5.0	0.000	0.000	1.0
12	0.09	0.29	0.06	0.0	5.0	5.558	2.614	1.5
13	0.09	0.27	0.3	0.5	5.0	5.558	2.614	1.5
14	0.07	0.25	0.6	0.0	5.0	5.558	2.614	1.5
15	-	-	0.01	0.0	-	-	-	-
16	0.19	0.38	0.05	0.0	5.0	4.372	0.978	4.0
17	-	-	0.0024	0.0	-	-	-	-
18[+]	-	-	0.05	0.0	-	-	-	-

* a (m^{-1}) and b (m^{-1}) are Coefficients in vegetation root distribution equation, d_r (m) is the depth of rooting zone that contains 99% of the roots. [+] type 18 is the purely bare soil, the albedoes are calculated based on the color and soil wetness.

(iii) Physiological properties

All physiological parameters are taken as constant and independent of vegetation types in the current version.

α	Quantum efficiency at 25°C	(0.06 μmol μmol^{-1})
K_{o25}	O_2 michaelis-menten constant at 25°C	(30000 pa)
K_{c25}	CO_2 michaelis-menten constant at 25°C	(30 pa)
$V_{max\,25}$	Maximum rate of carboxylation at 25°C	(33 μmol $m^{-2}s^{-1}$)
a_{ko}	Temperature sensitivity parameter for K_{o25}	(1.2)
a_{kc}	Temperature sensitivity parameter for K_{c25}	(2.1)
a_{vmax}	Temperature sensitivity parameter for $V_{max\,25}$	(2.4)
b	Minimum leaf conductance	(2000 μmol $m^{-2}s^{-1}$)
m	Slope for conductance-to-photosynthesis relationship	(9)

(b) Time-Varying Parameters

F_{veg}	Fraction of vegetation cover
L_{AI}	Leaf area index ($m^2\,m^{-2}$)
S_{AI}	Stem area index ($m^2\,m^{-2}$)

The interactive ecosystem dynamics submodel was not included in the current version. Thus, for off-line studies, the site observed F_{veg}, L_{AI} and S_{AI} should be used; for regional and global modelling studies, global data from satellites or field survey should be used (see section 2.6). In our mosaic treatment, F_{veg} is 100% for all vegetated tiles.

2.5 *Atmospheric Forcing Data*

The atmospheric boundary conditions necessary to force CLM include the following:

z_r Observational height of wind (or height of the lowest atmospheric model level) (m)

z_h Observational height of air temperature (m)

z_q Observational height of air humidity (m)

u_s Lowest model level west to east wind component (m s^{-1})

v_s Lowest model level south to north wind component (m s^{-1})

T_a Lowest model level air temperature (K)

q_a Lowest model level water-vapor specific humidity (kg kg^{-1})

P Precipitation rate (mm s^{-1})

$S^{\downarrow}_{\Lambda,\mu}$ Components of the incident solar radiation: visible (beam and diffuse) and near-infrared (beam and diffuse) (W m^{-2})

$L^{\downarrow}_a$ Incident atmospheric long-wave radiation (W m^{-2})

p_l Lowest model level air pressure (pa)

p_s Surface air pressure (pa)

2.6 *Prognostic Variables*

(a) State variables:
Each land surface title has 6 prognostic variables. Two are associated with the energy balance equations (Eq. 4.21 and Eq. 4.31):

T_c Canopy temperature (K)

T_j Temperature at the j^{th} node of soil or snow (K)

Four are associated with the water balance equations (Eq. 3.7 – 3.13):

w_{dew} Canopy interception water store (mm)

$w_{liq,j}$ Mass of water within the j^{th} layer of soil or snow (kg m^{-2})

$w_{ice,j}$ Mass of ice within the j^{th} layer of soil or snow (kg m^{-2})

Δz_j Snow layer thickness (j = snl+1, ...,-1, 0)

where snl is the number of snow layer (negative). Here, the mass of liquid and solid water within snow or soil layers is given by two variables separately, and the thickness of snow layers is taken as a state variable.

The model state variables are required the initialization. The observational initial values are the first choice. If observational initial data are not available, arbitrarily assigned initial fields, and then spined up the first model year to equilibrium state, and take the equilibrium state variables as the initial values. The arbitrary initial data are created following the rule:

- Foliage temperature is initially set to lowest atmospheric model air-temperature.
- Canopy water storage set to zero.

- Soil temperatures are initialized as in bucket type parameterizations using the lowest atmospheric model air-temperature and a climatological deep-ground temperature.
- Soil moistures are initialized to a percentage of field capacity. The percentage of liquid water and ice lens is estimated from the layer temperature.
- If the depth of snow is known, subdivide the snow pack up to five layers which follows the rule: the minimum thickness from top layer to bottom layer 0.010, 0.015, 0.025, 0.055, 0.115 (m), and with maximum thickness of 0.02, 0.05, 0.11, 0.23, and the value greater that 0.23 m, the snow layer temperature set to surface air temperature, if air temperature is greater than freezing point, set to 273.16 K. If no any information on snow is available, all snow related variables are set to 0, except snow mass is initially set to 5×10^4 kg m^{-2} for areas of permanent land ice.

(b) Derived variables to atmospheric model:

LE	Latent heat flux (W m^{-2})
H	Sensible heat flux (W m^{-2})
τ_x	Zonal momentum flux (kg m^{-1}s^{-2})
τ_y	Meridional momentum flux (kg m^{-1}s^{-2})
$\underline{E}$	Water flux (kg m^{-2}s^{-1})
$\overline{\alpha}_{\lambda,\mu}$	Surface albedo [visible (direct, diffuse), near-infrared (direct, diffuse)]
$L_g^{\uparrow}$	Outgoing longwave radiation from surface (W m^{-2})

The land and atmosphere are assumed to be explicitly coupled in the code; i.e., the current state of atmosphere is used to force the land model, and surface fluxes and albedo are then used to update the atmosphere.

2.7 *Data and interface requirements for CLM coupled CCSM*

(Expected to be done by NCAR people)

[
All vegetation data are derived from the global 1 km $\times$1 km IGBP land cover and fractional vegetation cover data as well as the global 8 km $\times$ 8 km green leaf area index data. These data are discussed in detail in Zeng et al. (2001).

Soil color types are taken from the BATS T42 data set for use with CCM.

Sand, silt, and clay data were taken from LSM (Bonan 1996), which were derived from Webb et al.'s (1993) $1.0^0\times1.0^0$ data.

Inland water and permanent wetland data are derived from the global 1 km IGBP land cover data (see Zeng et al. 2001). Wetland "soil" is treated as saturated soil when calculating temperatures.
]

3. Water Balance

3.1 *Equations*

(1) Integral form of mass conservation equations:
Within a control volume ΔV, the time rate of change in mass of water must be equal to the net flow across the boundary surface S and its rate of internal production. The integral form of mass conservation of water phase k is written as,

$$\frac{\partial}{\partial t}\int_{\Delta V}\rho_k\theta_k dV = -\int_S U_k \cdot dS + \sum_{k'}\int_{\Delta V} M_{k'k}(1-\delta_{k'k})\,dV + \int_{\Delta V} S_k\,dV \qquad (3.1)$$

Time rate of mass change | Mass flow | Phase change | Sources or sinks

where

ρ_k Intrinsic density of constituent k (kg m^{-3}),
θ_k Partial volume of constituent k ($m^{-3}m^{-3}$),
U_k Mass flux (kg $m^{-2}s^{-1}$),
$M_{k'k}$ Phase change from phase k' to phase k (kg $m^{-3}s^{-1}$),
$\delta_{k'k}$ Kronecker delta,
S_k Source or sink term
($k = d,\ i,\ l,\ v$ for dry soil, ice, liquid and vapor)

(2) Vertical discretization
(a) Soil
CCM-like vertical differencing is used, in which mesh points are specified and interfaces are located half way between two neighbor layers (Figure 3.1). The depth of soil layer j^{th} at the node depth, z_j (m), is defined as,

$$z_j = 0.025\times\{\exp[0.5(j-0.5)]-1\},\ (j = 1, 2,...,msl) \qquad (3.2)$$

where j is node index (in increasing order from top to bottom), and "msl" is the index of bottom soil layer. The thickness of each layer, Δz_j (m), is

$$\Delta z_j = \begin{cases} 0.5(z_1+z_2), & j=1 \\ 0.5(z_{j+1}-z_{j-1}),\ j=2,3,...,msl-1 \\ (z_j - z_{j-1}), & j=msl \end{cases} \qquad (3.3)$$

The depth at the interface, $z_{h,j}$ (m), is

$$z_{h,j} = \begin{cases} 0, & j=0 \\ 0.5(z_j+z_{j+1}),\ j=1,2,...,msl-1 \\ z_j + 0.5\Delta z_j, & j=msl \end{cases} \qquad (3.4)$$

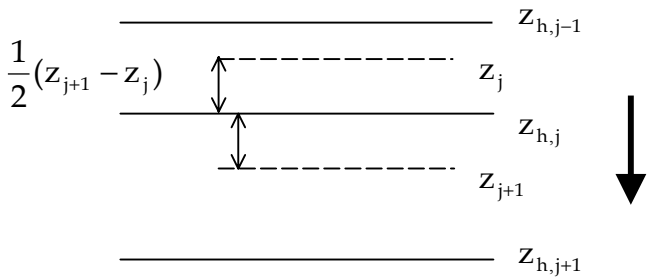

Figure 3.1. Schematic diagram of the vertical finite-discretization of soil layer.

(b) Snow

The snow-pack is modeled with up to 5 layers depending upon the total snow depth. Contrary to usual practice, the layers from top to bottom are numbered as negative values from "snl"+1, ...,-1, 0, which permits the accumulation or ablation of snow at the top of the snow cover without renumbering the layers. The vertical discretization will be given in section 5. The node is located at the mid-point of a layer and the depths of nodes and layer interfaces from soil surface are also defined as negative values:

$$z_j = z_{h,j+1} - 0.5\Delta z_j, \ (j = 0, ..., snl+1) \tag{3.5}$$

$$z_{h,j} = z_{h,j+1} - \Delta z_{j+1}, \ (j = -1, ..., snl) \tag{3.6}$$

where thickness Δz_j is positive and the absolute value of "snl" is the total number of snow-pack differencing.

(3) Water conservation equations for canopy, soil and snow

Integration of equation (3.1) over the control volumes (canopy, soil and snow layers) (with the assumptions of horizontally homogeneous and water vapor negligible) yields:

(a) Canopy water

$$\frac{\partial w_{dew}}{\partial t} = \sigma_f P - D_d - D_r - E_w \tag{3.7}$$

(b) Snow water and ice

$$\frac{\partial w_{liq,\,j}}{\partial t} = [q_{j-1} - q_j] + [M_{il}\Delta z]_j - \rho_l \theta_j \Delta z_j \left[\frac{1}{\Delta z}\frac{\partial \Delta z}{\partial t}\right]_j \tag{3.8}$$

$$\frac{\partial w_{ice,\,j}}{\partial t} = [q_{j-1(ice)} - q_{j(ice)}] - [M_{il}\Delta z]_j \tag{3.9}$$

(c) Soil water and ice

$$\frac{\partial w_{liq,\,j}}{\partial t} = [q_{j-1} - q_j] - f_{root,j*}E_{tr} + [M_{il}\Delta z]_j \tag{3.10}$$

$$\frac{\partial w_{ice,\,j}}{\partial t} = [q_{j-1(ice)} - q_{j(ice)}] - [M_{il}\Delta z]_j \tag{3.11}$$

where w_{liq} and w_{ice} are the liquid and ice mass (kg m^{-2}) in layers respectively, and

$$w_{liq,\,j} = \rho_l[\theta_l \Delta z]_j \tag{3.12}$$

$$w_{ice,\,j} = \rho_i[\theta_i \Delta z]_j \tag{3.13}$$

where θ_l and θ_i are the partial volumes of liquid and solid water ($m^3\ m^{-3}$) respectively, ρ_l and ρ_i are the intrinsic densities of liquid and solid water (kg m^{-3}) respectively.

3.2 *Vegetation storage of intercepted precipitation and dew*

Precipitation arriving at the vegetation top is either intercepted by foliage, or directly falls through the gaps of leaves to ground. The rate of direct through-fall is given by,

$$D_d = [\sigma_f \exp(-0.5 L_{SAI})]P \tag{3.14}$$

which is similar to the treatment of the transmission of solar beam for spherically distributed leaves.

The rate of drainage (outflow of the water stored on foliage and stem) is given by:

$$D_r = \begin{cases} \dfrac{w_{dew} - w_{dmax}}{\Delta t}, & \text{when } w_{dew} > w_{dmax} \\ 0, & \text{when } w_{dew} \le w_{dmax} \end{cases} \tag{3.15}$$

Maximum water capacity of canopy:

$$w_{d\max} = 0.1\,\text{mm} \times \sigma_f L_{SAI} \tag{3.16}$$

The maximum storage of solid water is assumed to be the same as that of liquid water (Dickinson et al. 1993, page 47).

3.3 *Evaporation from ground*

(a) Evaporation from bare ground

$$E_{g(soil)} = \rho_a \frac{q_g - q_a}{r_d} \tag{3.17}$$

where r_d is the aerodynamic resistance (s m^{-1}) for evaporation between the atmosphere at reference height z_q and the soil surface, q_a is the specific humidity at height z_q, and q_g is specific humidity at soil surface:

$$q_g = h_r q_{sat}(T_1) = \exp\left(\frac{\psi g}{R_w T_1}\right) \times q_{sat}(T_1) \tag{3.18}$$

The above formulation from Philip (1957) has some known deficiencies (e.g., Mahfouf and Noilhan 1991, Kondo and Saigusa 1990). One deficiency is that gradient $\partial h_r / \partial \theta$ will become too large near soil potential $\psi = -2 \times 10^5$ mm so that a small increase of soil moisture will cause $h_r + \dfrac{\partial h_r}{\partial \theta} \Delta\theta > 1$. Additional research is needed to develop a better formulation in the future.

Using the suction for ψ in section 3.5, the derivative $\partial E_g / \partial \theta_1$ (which is used in section 3.5) can be obtained:

$$\frac{\partial E_g}{\partial \theta_1} = \left[\rho_a \frac{q_{sat}(T_1)}{r_d} \right] \frac{\partial h_r}{\partial \theta_1} = S_d \Delta z_1 \tag{3.19}$$

$$S_d = -\left[\rho_a \frac{q_{sat}(T_1)}{r_d} \right] \times h_r \frac{B\psi_1 g}{R_w T_1 \theta_1 \Delta z_1}$$

For numerical reason, a limitation for $\partial h_r / \partial \theta$ is added:

$$h_r + \frac{\partial h_r}{\partial \theta} \Delta\theta \le 1 \;\Rightarrow\; \frac{\partial h_r}{\partial \theta} \le \frac{1 - h_r}{1 - \theta_d - \theta_i}$$

(b) Evaporation from snow surface

$$E_{g\,(snow)} = \rho_a \frac{q_{sat}(T_{snl+1}) - q_a}{r_d} \tag{3.20}$$

where $q_{sat}(T_{snl+1})$ is the saturated specific humidity at temperature T_{snl+1}.

3.4 *Runoff and infiltration*

Parameterization of runoff-related processes in soil vegetation-atmosphere transfer (SVAT) schemes has been an active research topic. There is an increasing awareness that the parameterization needs to explicitly account for the topographic control on the soil moisture distribution and runoff generation. Recently, attempts have been made to incorporate TOPMODEL into SVAT schemes (Stieglitz et al. 1997).

The form of TOPMODEL used here in CLM is similar only in concept to the standard TOPMODEL equations. First, basic TOPMODEL concepts are introduced into CLM. This approach assumes an exponential decrease of saturated hydraulic conductivity, from which a water table level is determined and the partial contributing area is computed. Runoff is parameterized from the lowlands in terms of precipitation incident on wet areas and a base flow. The CLM with this approach has been tested in the beta-testing stage with data from the Red-Arkansas River basins of the Southern Great Plains of the USA. Modeled runoff is too low, while the evapotranspiration is too high. The main causes are that the simulated water table level is too deep and is not sufficiently sensitive to the soil moisture content.

Subsequently an improved approach is developed to determine the water table depth so that it can vary from the bottom of the model soil column to the surface depending on the soil moisture content in all the model layers. In addition to runoff over saturated areas, surface and subsurface runoff components are allowed to occur over the areas outside the wetland following the BATS method (Dickinson et al., 1993). The simulated runoff shows improved agreement with data from the Red-Arkansas River basins. A detailed description of the above runoff implementation, as used in the current CLM, is given below.

CLM assumes an exponential decrease of the saturated hydraulic conductivity according to

$$K_{sat} = K_{sat,0} \exp(-z / z_*) \tag{3.21}$$

where K_{sat} is the saturated hydraulic conductivity at depth z, $K_{sat,0}$ is the saturated hydraulic conductivity at the surface, and z_* (=500 mm) is the length scale for the K_{sat} decrease.

Following Stieglitz et al. (1997), a watershed or a grid box in atmospheric models is divided into two zones (saturated and unsaturated). The fraction of the watershed that is saturated (the partial contributing area), f_{sat}, is parameterized as follows,

$$f_{sat} = w_{fact} \exp(-z_w) \tag{3.22}$$

where w_{fact} is a parameter determined by the distribution of the topographic index (=0.3 in the current version), and z_w is the mean water table depth (dimensionless) which is given by

$$z_w = f_z(z_{bot} - \sum_{j=1,N} s_j \Delta z_j) \tag{3.23}$$

where f_z is a water table depth scale parameter (=1 m^{-1}), z_{bot} is the bottom depth of the lowest soil layer, s_j is soil wetness at layer j, and Δz_j is soil layer thickness at layer j. The above equation states that the water table is at the surface when the soil is saturated, and at the bottom when the soil is dry.

Both surface runoff, R_s, and base flow, R_b, are computed for saturated and unsaturated regions separately according to

$$R_s = (1 - f_{sat}) R_{s,1} + f_{sat} R_{s,2} \tag{3.24}$$

$$R_b = (1 - f_{sat}) R_{b,1} + f_{sat} R_{b,2} \tag{3.25}$$

and

$$R_{s,1} = \overline{w}_s{}^4 G_w$$

$$R_{s,2} = G_w$$

$$R_{b,1} = K_D \overline{w}_b^{(2B+3)}$$

$$R_{b,2} = 1_b \exp(-z_w)$$

where G_w is effective rainfall (throughfall plus drip from the canopy) plus snowmelt. When snow completely covers the ground, G_w is equal to melt water from the bottom of the snowpack. $\overline{w}_s$ is the soil layer thickness weighted soil wetness in the top three layers, while $\overline{w}_b$ is the soil layer thickness and hydraulic conductivity weighted soil wetness in the bottom five layers. K_D is the saturated soil hydraulic conductivity for the bottom layers contributing to the base flow, and is used as a tuning parameter in CLM ($K_D = 4 \times 10^{-2}$ mm s^{-1} according to the Red-Arkansas watershed stream flow data). 1_b is a base flow parameter for the saturated fraction of the watershed, and may be estimated from soil and topographic features. In CLM, $1_b = 1 \times 10^{-5}$ mm s^{-1}.

The liquid soil water within each layer of the total soil column is checked every time step to ensure that it does not exceed its maximum effective amount. If the excess does occur,

it is added to the total runoff and the liquid soil water content in the relevant layer is set to its maximum effective value. Thus, the total runoff is

$$R_{tot} = R_s + R_b + R_{excess} \tag{3.26}$$

The infiltration, q_{infl}, is defined as a residual of the surface water balance,

$$q_{infl} = G_w - E_{soil} - R_s \tag{3.27}$$

where E_{soil} is soil surface evaporation (mm s^{-1}).

Overall, the present approach can produce a global mean runoff within observed ranges. Work is under way to follow more closely the TOPMODEL equations and to estimate the topographic statistics explicitly based on high-resolution topography data on global scales.

3.5 *Soil water*

For convenience, millimeter (rather than meter) is used as the length unit in soil water calculation only.

3.5.1 Water flow in unfrozen soil and frozen soil

Darcy's law is used to calculate soil moisture:

$$q = -K\left(\frac{\partial \psi}{\partial z} - 1\right) \tag{3.28}$$

where q is the water flow within soil (kg $m^{-2}s^{-1}$) and the positive value point from surface to bottom; K and ψ are the hydraulic conductivity and matric potential of soil respectively, which vary with θ and soil texture based on the Clapp and Hornberger (1978).

(a) Hydraulic conductivity of soil K:

$$K = K_{sat} s^{2B+3} \tag{3.29}$$

where the wetness (liquid water degree of saturation) is defined as

$$s = \left[\frac{\theta_l}{1 - \theta_d - \theta_i}\right]$$

For numerical reason, when effective porosity ($1 - \theta_d - \theta_i$) is less than 0.05 in any of two neighboring layers or liquid content less than 0.001, $K = 0$.

(b) Matric potential of soil ψ:

The matric potential of the unfrozen soil is written as:

$$\psi = \psi_{sat} s^{-B} \tag{3.30}$$

The matric potential of the frozen soil is assumed to be related to temperature only (Fuchs et al. 1978):

$$\psi = 1. \times 10^3 \times \frac{L_f}{g} \times \frac{T - 273.16}{T} \quad \text{(mm)} \tag{3.31}$$

where L_f is the latent heat of fusion of ice (J kg^{-1}), g is the gravitational acceleration (m s^{-2}).

3.5.2 Numerical scheme

Soil water equation (3.10) is re-written as,

$$\frac{\Delta z_j}{\Delta t}\Delta\theta_j = [q_{j-1}^{n+1} - q_j^{n+1}] - f_{root,j*}E_{tr} \tag{3.32}$$

where $\Delta\theta_j = \theta_j^{n+1} - \theta_j^n$ and superscript n is time-step. The water flow q (eq. 3.32) at the depth $z_{h,j}$ of the interface between layer j and layer $j+1$ is written with difference form as follows,

$$q_j = -K_j \frac{(\psi_{j+1} - \psi_j) - (z_{j+1} - z_j)}{z_{j+1} - z_j} = -K_j\phi_{j*} \tag{3.33}$$

In the above equation and in the rest of this report, the following notation is used for simplicity:

$$\varphi_{j*} = \frac{(\psi_{j+1} - \psi_j) - (z_{j+1} - z_j)}{z_{j+1} - z_j}$$

$$K_{j*} = \frac{K_j}{z_{j+1} - z_j}$$

The matric potential and its partial derivatives at the node depth z_j are

$$\psi_j = \psi_{sat}\left[\frac{\theta_j}{\theta_{sat,j}}\right]^{-B} \tag{3.34}$$

$$\frac{\partial\psi_j}{\partial\theta_j} = -\left[\frac{B}{\theta_j}\right]\psi_j \tag{3.35}$$

The hydraulic conductivity and its partial derivatives at the depth $z_{h,j}$ are

$$K_j = K_{sat}(z_{h,j})\left[\frac{\theta_j(z_{h,j} - z_j) + \theta_{j+1}(z_{j+1} - z_{h,j})}{\theta_{sat,j}(z_{h,j} - z_j) + \theta_{sat,j+1}(z_{j+1} - z_{h,j})}\right]^{2B+3} \tag{3.36}$$

$$\frac{\partial K_j}{\partial\theta_j} = \frac{\partial K_j}{\partial\theta_{j+1}} = K_j\frac{2B+3}{\theta_j + \theta_{j+1}} \tag{3.37}$$

for j = 1, 2, ..., msl-1

and

$$K_j = K_{sat}(z_{h,j})\left[\frac{\theta_j}{\theta_{sat,j}}\right]^{2B+3}$$

$$\frac{\partial K_j}{\partial\theta_j} = K_j\frac{2B+3}{\theta_j}$$

for j = msl

(3.32) can be written as a tridiagonal matrix for layer volumetric content:

$$a_j\theta_{j-1}^{n+1} + b_j\theta_j^{n+1} + c_j\theta_{j+1}^{n+1} = r_j \qquad (3.38)$$

where

$$a_j = -\left[\frac{\partial q_{j-1}}{\partial \theta_{j-1}}\right]$$

$$b_j = \left[\frac{\Delta z_j}{\Delta t} - \frac{\partial q_{j-1}}{\partial \theta_j} + \frac{\partial q_j}{\partial \theta_j}\right]$$

$$c_j = \left[\frac{\partial q_j}{\partial \theta_{j+1}}\right]$$

$$r_j = [q_{j-1}^n - q_j^n] - f_{root,j*}E_{tr}$$

and

$a_j = 0$, for j = 1

$c_j = 0$, for j = msl

(a) At surface, $z_{h,j} = 0$,

$$q_0^{n+1} = q_0^n + \frac{\partial q_0}{\partial \theta_1}\Delta\theta_1$$

For the case of bare soil,

$$q_0 = \sigma_f P + D_d + D_r + S_m - E_g - R_{unoff}$$

$$\frac{\partial q_0}{\partial \theta_1} = -\frac{\partial E_g}{\partial \theta_1}$$

$$\frac{\partial q_0}{\partial \theta_1} = S_d \Delta z_1$$

For the case of snow covered soil,

$$q_0 = S_m - R_{unoff}$$

$$\frac{\partial q_0}{\partial \theta_1} = 0$$

(b) At the interior interface $z_{h,j}$ (j = 1,..., msl-1),

$$q_j = -K_j\phi_{j*}$$

$$q_j^{n+1} = q_j^n + \frac{\partial q_j}{\partial \theta_j}\Delta\theta_j + \frac{\partial q_j}{\partial \theta_{j+1}}\Delta\theta_{j+1}$$

$$\frac{\partial q_j}{\partial \theta_j} = -\left[K_{j*}\frac{\partial}{\partial \theta_j}(-\psi_j) + \frac{\partial K_j}{\partial \theta_j}\varphi_{j*}\right]$$

$$\frac{\partial q_j}{\partial \theta_{j+1}} = -\left[K_{j*} \frac{\partial}{\partial \theta_{j+1}} (\psi_{j+1}) + \frac{\partial K_j}{\partial \theta_{j+1}} \varphi_{j*} \right]$$

(c) At the bottom $z_{h,j}$ (j = msl),

$$q_j = K_j$$

$$q_j^{n+1} = q_j^n + \frac{\partial q_j}{\partial \theta_j} \Delta \theta_j$$

$$\frac{\partial q_j}{\partial \theta_j} = \frac{\partial K_j}{\partial \theta_j}$$

3.6 *Snow water*

Surface layer (j = snl+1):

$$w_{ice,j}^{n+1} = w_{ice,j}^n + [P_s - E_{g(s)}]\Delta t \tag{3.39}$$

$$w_{liq,j}^{n+1} = w_{liq,j}^n + [P_r - E_{g(e)}]\Delta t \tag{3.40}$$

where $E_{g(s)}$ and $E_{g(e)}$ is the rate of sublimation (or freezing) and evaporation (condensation) (kg $m^{-2}s^{-1}$), respectively. P_s and P_r are precipitation of solid and liquid parts.

The water flow in snow layers:

$$q_j = 10^3 \times [\theta_l - s_r(1-\theta_i)]_j \Delta z_j \le 10^3 \times [1 - \theta_i - \theta_l]_{j+1} \Delta z_{j+1} \tag{3.41}$$

where s_r is the irreducible water in snow (0.033). When the porosity ($1-\theta_i$) of one of that of two neighboring layers is less that 0.05, the zero flow is assumed, i.e., $q_j = 0$. The snow water is given by

$$w_{liq,j}^{n+1} = w_{liq,j}^n - [q_{j-1} - q_j]\Delta t \tag{3.42}$$

3.7 *Effective root fraction and maximum transpiration*

(a) Effective root fraction $f_{root,j*}$ within layer j

$$f_{root,j*} = \frac{f_{root,j} w_{LT}[j]}{\sum f_{root,j} w_{LT}[j]} \tag{3.43}$$

$$w_{LT}[j] = \frac{\psi_{max} - \psi_j}{\psi_{max} - \psi_{sat}} \tag{3.44}$$

where $f_{root,j}$ is the root fraction within soil layer j, ψ_{max} is the maximum value of negative of potential of leaves before desiccation (-1.5×10^5 mm). The factor $w_{LT}[j]$ ranges from 0 at the permanent wilting point to 1 at saturation.

(b) Maximum transpiration rate E_{trmax}

The transpiration rate must be consistent with the maximum transpiration that the vegetation can sustain as defined below. When E_{tr} is found to exceed E_{trmax}, then r_s is re-determined so that $E_{tr} = E_{tr\,max}$, the formulation of the maximum transpiration is taken from BATS (Dickinson et al. 1993) as

$$E_{trmax} = 2\times10^{-4} \times \sigma_f L_{AI} \times \sum f_{root,j} w_{LT}[j] \quad (\text{kg m}^{-2}\text{s}^{-1}) \tag{3.45}$$

4. Energy Balance

4.1 *Equations*

Analogous to the conservation equation for mass (eq. 3.1), the conservation of energy stipulates that the time rate of change in stored energy within volume ΔV equal the net energy flux across the volume surface S. The terminology "energy balance " in effect describes a "heat balance", Since other source of energy (such as macrokinetic, chemical and viscous dissipation) are of a lower order and are customarily discounted. The amount of heat associated with a unit of mass at temperature relative to a reference level T_f is expressed in terms of its specific enthalpy, which for an isobaric system is the heat required raising or lowering the temperature to T from T_f. If the freezing point of water is chosen for T_f (=273.16 K), the specific enthalpy for three water phases and dry soil are,

$$h_i = c_i(T - T_f)$$
$$h_l = c_l(T - T_f) + L_f$$
$$h_v = L_s$$
$$h_d = c_d(T - T_f)$$

Specific heat at frozen point T_f,

$c_i = 2117.27$ $Jkg^{-1}K^{-1}$

$c_l = 4188.0$ $Jkg^{-1}K^{-1}$

c_d for dry soil (given by Equation 4.23)

Latent heat,

$L_f = 0.3336\times10^6$ Jkg^{-1}, latent heat of fusion

$L_s = 2.844\times10^6$ Jkg^{-1}, latent heat of sublimation

$L_v = 2.5104\times10^6$ Jkg^{-1}, latent heat of evaporation

Expressing the conductive flux by Fourier's law, where λ is the thermal conductivity of the medium ($W\ m^{-1}K^{-1}$), and denoting radiation flux as R ($W\ m^{-2}$), the integral form of energy equation is written as,

$$\frac{\partial}{\partial t}\sum_{k=i,l,v,d}\int_{\Delta V}\rho_k\theta_k h_k dV = -\sum_{k=i,l,v}\int_S U_k h_k \cdot dS + \int_S \lambda\nabla T \cdot dS + \int_{\Delta V} R dV \qquad (4.1)$$

Rate of change in stored heat — Convection — Conduction — Radiation

Assumption I:
Convective heat transfer is assumed to be negligible within canopy and soil and snow layers.

Assumption II:

Vaporization and sensible heat transfer are assumed to be negligible within snow and soil layers.

Assumption III:
Heat conductance is assumed to be negligible within canopy.

With these assumptions, the energy equation (4.1) becomes

$$\sum_{k=i,l,d}[\rho_k c_k \theta_k]_j \Delta z_j \frac{\partial T_j}{\partial t} = R_{n,j} - [L_f M_{il} \Delta z]_j - H - L_v E + \left[\lambda \frac{\partial T}{\partial z}\right]_{z_{h,j-1}}^{z_{h,j}} \tag{4.2}$$

4.2 *Leaf temperature and fluxes*

(1) Fraction of the leaves covered with water
The wetted fraction of the canopy is (Dickinson et al. 1993),

$$\tilde{L}_w = (w_{dew} / w_{dmax})^{2/3} \tag{4.3}$$

The dry fraction of foliage surface free to transpire is then defined by

$$L_d = (1 - \tilde{L}_w) L_{AI} / L_{SAI} \tag{4.4}$$

(2) Foliage laminar boundary resistance
The conductance for heat and vapor flux from leaves is given by

$$r_b^{-1} = C_f \times (U_{af} / D_f)^{1/2} \tag{4.5}$$

where $C_f = 0.01\ m\,s^{-1/2}$, D_f is the characteristic dimension of leaves in the direction of wind flow, U_{af} is the magnitude of the wind velocity incident on the leaves

$$U_{af} = |V_a| C_D^{1/2} = |V_a|^{1/2} r_{am}^{-1/2} \tag{4.6}$$

(3) Foliage fluxes
The air within the canopy has negligible heat capacity so that heat flux from the foliage H_c and from the ground H_g must be balanced by heat flux to the atmosphere H_a, i.e.,

$$H_a = H_c + H_g \tag{4.7}$$

The flux to the atmosphere is given by (Dickinson et al. 1993)

$$H_a = \sigma_f \rho_a c_p r_{ah}^{-1} (T_{af} - \theta_a) \tag{4.8}$$

The flux from the soil under the canopy is given by

$$H_g = \sigma_f \rho_a c_p C_{soilc} u_{af} (T_g - T_{af}) \tag{4.9}$$

where C_{soilc} is the transfer coefficient between the canopy air and underlying ground, and is assumed to be 0.004.

The heat flux from the foliage is

$$H_c = \sigma_f L_{SAI} \rho_a c_p\, r_b^{-1} (T_c - T_{af}) \tag{4.10}$$

Equations (4.7 – 4.10) are solved for T_{af}, the temperature of air within canopy,

$$T_{af} = \frac{c_A^h \theta_a + c_F^h T_c + c_G^h T_g}{c_A^h + c_F^h + c_G^h} \tag{4.11}$$

where

$$c_A^h = \sigma_f r_{ah}^{-1}$$
$$c_F^h = \sigma_f L_{SAI}\, r_b^{-1}$$
$$c_G^h = \sigma_f C_{soilc} u_{af}$$

are conductances, to the atmosphere above the canopy, from foliage, and from the ground, respectively.

Similarly, the canopy air is assumed to have negligible water vapor storage so that the flux of water from canopy air E_a balances the fluxes from the foliage E_c and from the ground E_g, i.e.,

$$E_a = E_c + E_g \tag{4.12}$$

The flux of water from canopy air to atmosphere is given by

$$E_a = \sigma_f \rho_a r_{aw}^{-1} (q_{af} - q_a) \tag{4.13}$$

The flux from the ground:

$$E_g = \sigma_f \rho_a C_{soilc} u_{af} (q_g - q_{af}) \tag{4.14}$$

The water on wet foliage (leaves and stem) evaporates per unit-wetted area according to

$$E_f^{pot} = \rho_a r_b^{-1} (q_f^{sat} - q_{af}) \tag{4.15}$$

The flux of water from the wetted foliage is given

$$E_w = \sigma_f L_{SAI} [1 - \delta(E_f^{pot})(1 - \tilde{L}_w)] E_f^{pot} \tag{4.16}$$

where δ is a step function and one for positive and zero for zero or negative argument.

Transpiration occurs only over dry leaf surface and only outward,

$$E_{tr} = \sigma_f L_{SAI} \delta(E_f^{pot}) L_d \frac{r_b}{r_b + r_s} E_f^{pot} \le E_{trmax} \tag{4.17}$$

The flux of water from foliage (total) is given by

$$E_c = E_w + E_{tr} = \sigma_f L_{SAI} r'' E_f^{pot} \tag{4.18}$$

where

$$r'' = 1 - \delta(E_f^{pot}) \left(1 - \tilde{L}_w - L_d \frac{r_b}{r_b + r_s} \right) \tag{4.19}$$

where r_s is the stomatal resistance.

The equations (4.12 – 4.19) are solved to obtain q_{af}

$$q_{af} = \frac{c_A^w q_a + c_v^w q_f^{sat} + c_G^w q_g}{c_A^w + c_V^w + c_G^w} \tag{4.20}$$
$$c_A^w = \sigma_f r_{aw}^{-1}$$
$$c_v^w = r'' c_F^w,\ c_F^w = \sigma_f L_{SAI}\, r_b^{-1}$$

$$c_G^w = \sigma_f C_{soilc} u_{af}$$

(3) Leaf temperature

Foliage energy conservation gives

$$R_{n,c} - H_c - L_v E_c = 0 \tag{4.21}$$

The canopy temperature can be obtained by solving the equation (4.21) iteratively

$$R_{n,c} - H_c - L_v E_c + \left(\frac{\partial R_{n,c}}{\partial T_c} - \frac{\partial H_c}{\partial T_c} - L_v \frac{\partial E_c}{\partial T_c} \right) \times (T_c^{n+1} - T_c^n) = 0 \tag{4.22}$$

where partial derivatives can be approximated as

$$\frac{\partial R_{n,c}}{\partial T_c} = \frac{\partial L_{n,c}}{\partial T_c} = -4\sigma T_c^3$$

$$\frac{\partial H_c}{\partial T_c} = \rho_a c_p c_F^h \frac{c_A^h + c_G^h}{c_A^h + c_F^h + c_G^h}$$

$$\frac{\partial E_c}{\partial T_c} = \rho_a c_v^w \frac{c_A^w + c_G^w}{c_A^w + c_v^w + c_G^w} \frac{\partial q_f^{sat}}{\partial T_c}$$

4.3 *Soil and snow temperatures*

4.3.1 Heat capacity and thermal conductivity

(1) Soil

Volumetric heat capacity:

$$c = \rho_d c_d \theta_d + \rho_l c_l \theta_l + \rho_i c_i \theta_i, \text{ (J m}^{-3}\text{k}^{-1}\text{)} \tag{4.23}$$

The volumetric heat capacity of soil solids was given by Equation (2.1).

Thermal conductivity (Farouki, 1981):

$$\lambda = K_e (\lambda_{sat} - \lambda_{dry}) + \lambda_{dry}, \text{ (W m}^{-1}\text{K}^{-1}\text{)} \tag{4.24}$$

where λ_{dry} is the thermal conductivity for dry natural soil,

$$\lambda_{dry} = \frac{0.135\rho_d \theta_d + 64.7}{2700 - 0.947\rho_d \theta_d}, \text{ (W m}^{-1}\text{K}^{-1}\text{)} \tag{4.25}$$

λ_{sat} is the thermal conductivity for saturated soil,

$$\lambda_{sat} = \lambda_d^{\theta_d} \lambda_i^{1-\theta_d-\theta_l} \lambda_w^{1-\theta_d} \tag{4.26}$$

$\lambda_i = 2.2\,9$ (W m^{-1}K^{-1}), for ice

$\lambda_w = 0.57$ (W m^{-1}K^{-1}), for water

$1 - \theta_d$ = porosity

λ_d is the thermal conductivity of soil solids, which was given by Equation (2.2).

K_e is a function of the degree of saturation $S_r = (\theta_i + \theta_l)/(1 - \theta_d)$ and phase of the water. For unfrozen soils,

$$K_e = \begin{cases} 0.7 \log_{10} S_r + 1.0 & S_r > 0.05 \text{ coarse} \\ \log_{10} S_r + 1.0 & S_r > 0.1 \text{ fine} \end{cases} \quad (4.27)$$

and for frozen soils,

$$K_e = S_r$$

(2) Snow

Volumetric heat capacity,

$$c = \rho_l c_l \theta_l + \rho_i c_i \theta_i \quad (4.28)$$

Thermal conductivity,

$$\lambda = \lambda_a + (7.75 \times 10^{-5} \rho_s + 1.105 \times 10^{-6} \rho_s^2) \times (\lambda_i - \lambda_a), \text{ (W K}^{-1}\text{m}^{-1}\text{)} \quad (4.29)$$

where λ_a and λ_i are air and ice thermal conductivity, respectively. ρ_s is the snow density ($\rho_s = \rho_i \theta_i + \rho_l \theta_l$) [kg m^{-3}].

(3) Thermal conductivity at the interface of layers

Assuming that the heat flux from node j to the interface between j and $j+1$ equals the heat from the interface to node $j+1$, we have

$$\lambda_j \frac{T_m - T_j}{z_{h,j} - z_j} = \lambda_{j+1} \frac{T_{j+1} - T_m}{z_{j+1} - z_{h,j}} = \lambda(z_{h,j}) \frac{T_{j+1} - T_j}{z_{j+1} - z_j}$$

where T_m is the interface temperature and $\lambda(z_{h,j})$ is the thermal conductivity at the interface $z_{h,j}$ and is given by

$$\lambda(z_{h,j}) = \frac{\lambda_j \lambda_{j+1} [z_{j+1} - z_j]}{\lambda_j [z_{j+1} - z_{h,j}] + \lambda_{j+1} [z_{h,j} - z_j]} \quad (4.30)$$

4.3.2 Numerical scheme

$$[c_j \Delta z_j] \frac{T_j^{n+1} - T_j^n}{\Delta t} = \omega [F_j^n - F_{j-1}^n] + (1 - \omega)[F_j^{n+1} - F_{j-1}^{n+1}] \quad (4.31)$$

where

T_j Layer-averages temperature in layer j (K),

Δz_j Layer thickness (m),

ω Weighting coefficient in time domain (ω=0.5),

F_j Heat flux across the interface between layer j and j+1, and is computed as follows,

for interior interface (j = snl+2,..., msl-1),

$$F_j = \lambda(z_{h,j}) \frac{T_{j+1} - T_j}{z_{j+1} - z_j} \quad (4.32)$$

for bottom boundary, the heat conductance is assumed to be zero, (j = msl),

$$F_j = 0$$

for surface boundary (j = snl+1),

$$F_{j-1} = \omega F_{j-1}^n + (1-\omega)F_{j-1}^{n+1} = -h^{n+1} = -[h + \partial h / \partial T_j \times (T_j^{n+1} - T_j^n)]$$

$$h = R_{n,g} - H_g - L_{v(s)}E_g$$

For simplicity, we use the notation:

$$\lambda_{j*} = \frac{\lambda(z_{h,j})}{z_{j+1} - z_j}, \qquad (j = snl+1,...,msl-1)$$

$$c_{j*} = \frac{\Delta t}{c_j \Delta z_j}$$

The surface layer temperature computed in this way is the layer-averaged temperature and hence has a somewhat reduced diurnal amplitude compared with surface skin temperature. An accurate surface skin temperature is provided that compensates for this effect and numerical error by tuning the heat capacity of the top layer (through the adjustment of the layer thickness) to give an exact match to analytic solution for diurnal heating. The top layer thickness is given by

$$\Delta z_{j*} = 0.5[z_j - z_{h,j-1} + c_a(z_{j+1} - z_{h,j-1})], \ (j = snl+1)$$

where c_a is a tunable parameter, varying from 0 to 1, and is taken as 0.34 by comparing numerical solution with the analytical solution (Z.-L.Yang 1998, unpublished manuscript).

(4.31) can be written as a tri-diagonal matrix for layer temperature:

$$a_j T_{j-1}^{n+1} + b_j T_j^{n+1} + c_j T_{j+1}^{n+1} = r_j \qquad (4.33)$$

For surface layer (j = snl+1),

$$a_j = 0$$

$$b_j = 1 + c_{j*}[(1-\omega)\lambda_{j*} - \partial h / \partial T_j]$$

$$c_j = -(1-\omega)c_{j*}\lambda_{j*}$$

$$r_j = T_j^n + c_{j*}[h - \partial h / \partial T_j \times T_j^n + \omega F_j^n]$$

For interior layers (j = snl+2, ... ,msl),

$$a_j = -(1-\omega)c_{j*}\lambda_{j-1*}$$

$$b_j = 1 + (1-\omega)c_{j*}(\lambda_{j*} + \lambda_{j-1*})$$

$$c_j = -(1-\omega)c_{j*}\lambda_{j*}$$

$$r_j = T_j^n + \omega c_{j*}[F_j^n - F_{j-1}^n]$$

For bottom layer (j = msl),

$$a_j = -(1-\omega)c_{j*}\lambda_{j-1*}$$

$$b_j = 1 + (1-\omega)c_{j*}\lambda_{j-1*}$$

$$c_j = 0$$
$$r_j = T_j^n - \omega c_{j*} F_{j-1}^n$$

4.4 *Phase change*

If $T_j^{n+1} > T_f$ and $w_{ice,j} > 0$, or $T_j^{n+1} < T_f$ and $w_{liq,j} > 0$, the phase change will take place. The rate of phase change is assessed from the energy excess (or deficit) as changing T_j to freezing point, i.e., $T_j^{n+1} = T_f$. The excess or deficit energy is determined as follows:

Surface node (j = snl+1),

$$H_j = h + \partial h / \partial T_j \times (T_f - T_j^n) + \omega F_j^n + (1-\omega) F_j^{n+1} - c_{j*}^{-1}(T_f - T_j^n) \quad (4.34a)$$

Interior nodes (j = snl+2,...,msl),

$$H_j = \omega(F_j^n - F_{j-1}^n) + (1-\omega)(F_j^{n+1} - F_{j-1}^{n+1}) - c_{j*}^{-1}(T_f - T_j^n) \quad (4.34b)$$

The ice mass is re-adjusted as,

$$w_{ice,j}^{new} = \max(0, w_{ice,j}^{old} - H_j \Delta t / L_f), \text{ if } H_j > 0 \quad (4.35a)$$
$$w_{ice,j}^{new} = \min(w_{ice,j}^{old} + w_{liq,j}^{old}, w_{ice,j}^{old} - H_j \Delta t / L_f), \text{ if } H_j < 0 \quad (4.35b)$$

Because part of energy H_j may not be consumed, the energy and the temperature are recalculated as,

$$H_{j*} = H_j - L_f \{w_{ice,j}^{new} - w_{ice,j}^{old}\} / \Delta t \quad (4.36a)$$
$$T_j^{n+1} = T_f + c_{j*} H_{j*} / (1 - c_{j*} \partial h / \partial T_j) \text{ for surface node} \quad (4.36b)$$
$$T_j^{n+1} = T_f + c_{j*} H_{j*} \text{ for interior nodes} \quad (4.36c)$$

4.5 *Lake temperatures*

The calculation of lake temperatures has not undergone any further development but is directly adopted from the one-dimensional six-layer thermal stratification model in LSM (Bonan 1996) which, in turn, was based on the lake models of Henderson-Sellers (1985, 1986) and Hostetler and Bartlein (1990) and the coupled lake-atmospheric model of Hostetler et al. (1993, 1994).

$$\frac{\partial T}{\partial t} = \frac{\partial}{\partial z}\left[(k_m + k_e)\frac{\partial T}{\partial z}\right] + \frac{1}{c_w}\frac{d\phi}{dz} \quad (4.37)$$

where

T Lake temperature (K),

k_m Molecular diffusion coefficients ($m^2 s^{-1}$), and $k_m = k_w / c_w$,

k_e Eddy diffusion coefficients ($m^2 s^{-1}$),

k_w Thermal conductivity of water (W $m^{-1}K^{-1}$),
c_w Heat capacity of water (J $m^{-3}K^{-1}$),
ϕ Solar radiation heat source term (W m^{-2}).

The above equation is solved numerically to calculate temperature for six-layer deep or shallow lakes with the boundary conditions of zero heat flux at the bottom and the net flux of energy at surface F_0 (W m^{-2}):

$$F_0 = \beta S_{n,g} - (L_{n,g} + H_g + LE_g + M) \tag{4.38}$$

where
$S_{n,g}$ Solar radiation absorbed by the lake (W m^{-2}),
$L_{n,g}$ Net long-wave radiation (W m^{-2}),
H_g Sensible heat flux (W m^{-2}),
LE_g Latent heat flux (W m^{-2}),
M Snow melt (W m^{-2}),
β Fraction of solar absorbed in the surface layer.

Deep and shallow lakes differ in total depth. Deep lakes are 50 m deep, with thickness Δz_j of 1, 2, 4, 8, 25, 20 m. Shallow lakes are 10 deep, with thickness Δz_j of 0.5, 1.0, 1.5, 2.0, 2.5, 2.5 m. Shallow lakes also differ from deep lakes in that $k_e = 0$ and there is no convective mixing. This mean that shallow lake temperature are the same as that for soil using thermal conductivity and heat capacity of water (k_w, c_w) and allowing for absorption of solar radiation with depth.

The numerical solution of (Eq. 4.38) is resulted by a tridiagonal system as follows,

$$a_j T_{j-1}^{n+1} + b_j T_j^{n+1} + c_j T_{j+1}^{n+1} = r_j \tag{4.39}$$

For simple, we use the notation:

$$m_1 = \frac{\Delta z_{j-1}}{k_m + k_{e,j-1}} + \frac{\Delta z_j}{k_m + k_{e,j}}, (j > 1)$$

$$m_2 = \frac{\Delta z_j}{k_m + k_{e,j}} + \frac{\Delta z_{j+1}}{k_m + k_{e,j+1}}, (j < 6)$$

$$m_3 = \frac{\Delta t}{\Delta z_j}$$

For the surface layer $j = 1$,

$$a_j = 0,$$

$$b_j = 1 + \frac{m_3}{m_2}$$

$$c_j = -\frac{m_3}{m_2}$$

$$r_j = T_j^n + \frac{\phi_{j-1/2} - \phi_{j+1/2}}{c_w} m_3 + \frac{F_0}{c_w} m_3 - (T_j^n - T_{j+1}^n)\frac{m_3}{m_2}$$

For layers $1 < j < 6$ is,

$$a_j = -\frac{m_3}{m_1}$$

$$b_j = 1 + \frac{m_3}{m_1} + \frac{m_3}{m_2}$$

$$c_j = -\frac{m_3}{m_2}$$

$$r_j = T_j^n + \frac{\phi_{j-1/2} - \phi_{j+1/2}}{c_w} m_3 + (T_{j-1}^n - T_j^n)\frac{m_3}{m_1} - (T_j^n - T_{j+1}^n)\frac{m_3}{m_2}$$

For bottom layer, $j = 6$,

$$a_j = -\frac{m_3}{m_1}$$

$$b_j = 1 + \frac{m_3}{m_1}$$

$$c_j = 0$$

$$r_j = T_j^n + \frac{\phi_{j-1/2} - \phi_{j+1/2}}{c_w} m_3 + (T_{j-1}^n - T_j^n)\frac{m_3}{m_1}$$

The eddy diffusion coefficient $k_{e,j}$ ($m^2 s^{-1}$) is,

$$k_{e,j} = \begin{cases} \dfrac{k w_* z_j}{P_0(1 + 37R_j^2)} \exp(-k_* z_j), & \text{for unfrozen deep lake layers,} \\ 0, & \text{for shallow lakes or frozen deep lake layers} \end{cases} \tag{4.40}$$

where k is von Kárman constant, $P_0 = 1$ is the neutral value of the turbulent Prandtl number, z_j is the depth of layer j^{th}, the surface friction velocity is $w_* = 0.0012 u_2$ ($m\ s^{-1}$), and k_* varies with latitude ϕ as $k_* = 6.6\,|\sin\phi|^{1/2}\, u_2^{-1.84}$, u_2 is the 2-meter height wind speed ($m\ s^{-1}$) and $u_2 = \dfrac{u_*}{k}\ln\left(\dfrac{2}{z_{0m}}\right) \geq 1$, u_* is the friction velocity, z_{0m} is the roughness length for momentum. The Richardson number is

$$R_j = \frac{1}{20}\left[-1 + \left(1 + \frac{40N^2 k^2 z_j^2}{w_*^2 \exp(-2k_* z_j)}\right)^{1/2}\right] \tag{4.41}$$

where $N^2 = -\dfrac{g}{\rho_j}\dfrac{\partial \rho}{\partial z}$, ρ_j is the density of water, and $\dfrac{\partial \rho}{\partial z}$ is approximated as $(\rho_{j+1} - \rho_j)/(z_{j+1} - z_j)$. The density of water is, as in Hostetler and Bartlein (1990),

$$\rho_j = 1000\,(1 - 1.9549 \times 10^{-5}\,|\,T_j - 277\,|^{1.68}) \tag{4.42}$$

$\phi_{j-1/2}$ and $\phi_{j+1/2}$ are the solar radiation fluxes at the top ($z = z_j - \Delta z_j / 2$) and bottom ($z = z_j + \Delta z_j / 2$) of the j^{th} layer. For $z > z_a$, where z_a is the base of the surface absorption layer, the solar radiation at depth z is,

$$\phi(z) = 0.6 S_{n,g} \exp[-\eta(z - z_a)] \tag{4.43}$$

where η is the light extinction coefficient for water (for deep lakes $\eta = 0.1$, for shallow lakes $\eta = 0.5$), z_a is the base of the surface absorption layer (deep lake $z_a = 0.6$ m, shallow lakes $z_a = 0.5$ m).

5. Snow Compaction and Layer Combination and Subdivision

5.1 *Snow Compaction*

Snow compaction is mainly contributed by following four metamorphisms: destructive, pressure, constructive and melt metamorphism (Yen 1981). In the current version, only three of metamorphisms [destructive, overburden (or pressure), and melt] are implemented. The treatments of the former two are from SNTHERM.89 and SNTHERM.99 (1991), and the contribution due to melt metamorphism is simply taken as a ratio of snow ice fraction after the melting versus before the melting. The total fraction of the natural compaction rate is written as,

$$C_R = -\left[\frac{1}{\Delta z}\frac{\partial \Delta z}{\partial t}\right]_{\text{destructive}} - \left[\frac{1}{\Delta z}\frac{\partial \Delta z}{\partial t}\right]_{\text{overburden}} - \left[\frac{1}{\Delta z}\frac{\partial \Delta z}{\partial t}\right]_{\text{melt}} \tag{5.1}$$

and the layer thickness due to compaction is,

$$\Delta z_j = \Delta z'_j (1 + C_{R,j}\Delta t) \tag{5.2}$$

where $\Delta z'_j$ is the thickness of snow layer j^{th} before the calculation of compaction.

(1) Snow settling as a result of destructive metamorphism.
Immediately upon reaching the ground, snow begins a process of rapid change in which individual snowflakes quickly lose their original shape and metamorphose into more rounded forms. Branched crystals break down, either through the mechanical forces of wind or through thermodynamic stress, so that settling or grain packing of the snow pack occurs. For newer snow with densities of less than 100 kg m^{-3}, settling due to destructive metamorphism is important. New snow has a certain structural strength due to "cogging" between the crystal branches, which gives way as metamorphism proceeds. Anderson (1976) proposed the following empirical function for compaction at this stage:

$$-\left[\frac{1}{\Delta z}\frac{\partial \Delta z}{\partial t}\right]_{\text{destructive}} = -2.778\times 10^{-6} c_3 c_4 e^{-0.04(T_f - T)} \tag{5.3}$$

where

$c_3 = c_4 = 1$.

For the case $\rho_i \theta_i > 100$ (kg m^{-3})

$c_3 = e^{-0.046(\rho_i \theta_i - 100)}$ and $c_4 = 1$,

For the case $\rho_l \theta_l > 0.01$ (kg m^{-3})

$c_3 = 1$ and $c_4 = 2$,

Note that (5.3) predicts a deformation rate of 1% per hour for snow densities less than 100 kg m^{-3} and has an enhancement factor of two for wet snow.

(2) Compaction due to overburden.
As snow accumulates, the weight of overlying snow results in a further, more sustained, compaction of the snow cover. Stress from the overburden leads to an increased rate of bond growth, which in turn results in grain shape that packs more efficiently. After snow has undergone its initial settling stage, densification proceeds at a slower rate, which is largely determined by snow load or overburden. In the low stress range associated with

seasonal snow covers, the deformation rate is a linear function of the snow load pressure P_s such that

$$\left[\frac{1}{\Delta z}\frac{\partial \Delta z}{\partial t}\right]_{\text{overburden}} = -\frac{P_s}{9\times 10^5} e^{-0.08(T_f - T) - 0.023\rho_i \theta_i} \tag{5.4}$$

here P_s is the weight of the overlying snow (kg m^{-2})

(3) Compaction due to melt.
In the later stage of the melt period (i.e., after the snow has undergone several freeze-thaw cycles), this compaction process contributes to over-densification of the pack:

$$\left[\frac{1}{\Delta z}\frac{\partial \Delta z}{\partial t}\right]_{\text{melt}} = \frac{1}{\Delta t}\left[\frac{f_I^{n+1} - f_I^n}{f_I^n}\right] \tag{5.5}$$

where f_I is the fraction of ice relative to the total water content in a layer.

5.2 *Combination*

When a snow layer has totally melted or when its thickness is less than the prescribed minimum value, the layer will be combined with a neighboring layer. The top or bottom neighbor is selected as the recipient according to the following criteria:

(a) if the surface snow layer is removed, combine it with its bottom neighbor;
(b) if the bottom neighbor of the snow layer is soil, combine it with its overlying snow neighbor;
(c) if the snow layer has entirely melted, combine it with the underlying snow neighbor; and
(d) if none of the above applies, combine the snow layer with the thinner neighbor.

The minimum values of the five snow layers (from surface to bottom) are 0.010, 0.015, 0.025, 0.055, and 0.115 (m), respectively.

Mass and energy re-distribution
When two snow layers (denoted by j and $j+1$) are combined, their thickness combination is

$$\Delta z_{j^*} = \Delta z_j + \Delta z_{j+1} \tag{5.6}$$

the mass combination is

$$[w_{liq}]_{j^*} = [w_{liq}]_j + [w_{liq}]_{j+1} \tag{5.7}$$

$$[w_{ice}]_{j^*} = [w_{ice}]_j + [w_{ice}]_{j+1} \tag{5.8}$$

and temperature re-distribution is computed based on:

$$h_j = [c_i w_{ice} + c_l w_{liq}]_j \times [T_j - T_f] + L_f [w_{liq}]_j$$

$$h_{j+1} = [c_i w_{ice} + c_l w_{liq}]_{j+1} \times [T_{j+1} - T_f] + L_f [w_{liq}]_{j+1}$$

$$h_{j^*} = h_j + h_{j+1}$$

$$T_{j^*} = \begin{cases} T_f + h_{j^*} / [c_l w_{liq} + c_i w_{ice}]_{j^*}, & \text{for } h_{j^*} < 0 \\ T_f, & \text{for } h_{j^*} \le L_f [w_{liq}]_{j^*} \\ T_f - (h_{j^*} - L_f [w_{liq}]_{j^*}) / [c_l w_{liq} + c_i w_{ice}]_{j^*}, & \text{for } h_{j^*} > L_f [w_{liq}]_{j^*} \end{cases} \tag{5.9}$$

where subscript $_{j*}$ is the layer number index of the combined layer.

5.3 *Subdivision*

When the thickness of a layer exceeds the prescribed maximum thickness (from snow surface to bottom, 0.02[1], 0.05, 0.11, 0.23, and >0.23 m), the layer will be subdivided. The rule is shown in the figure 5.1, where d_{sn} is the total snow depth (m).

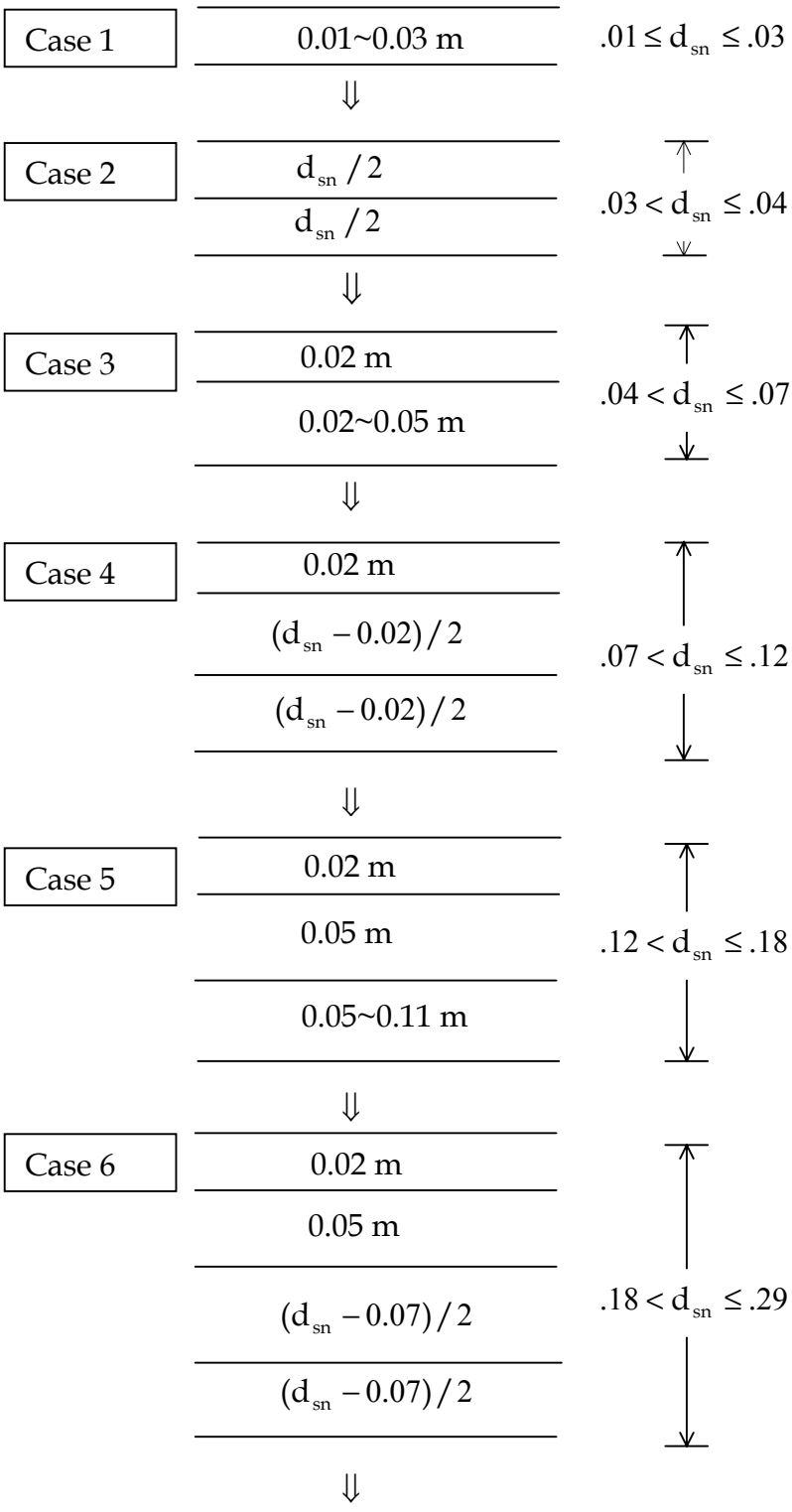
Case 1
0.01~0.03 m
$.01 \le d_{sn} \le .03$
Case 2
$d_{sn}/2$
$d_{sn}/2$
$.03 < d_{sn} \le .04$
Case 3
0.02 m
0.02~0.05 m
$.04 < d_{sn} \le .07$
Case 4
0.02 m
$(d_{sn} - 0.02)/2$
$(d_{sn} - 0.02)/2$
$.07 < d_{sn} \le .12$
Case 5
0.02 m
0.05 m
0.05~0.11 m
$.12 < d_{sn} \le .18$
Case 6
0.02 m
0.05 m
$(d_{sn} - 0.07)/2$
$(d_{sn} - 0.07)/2$
$.18 < d_{sn} \le .29$

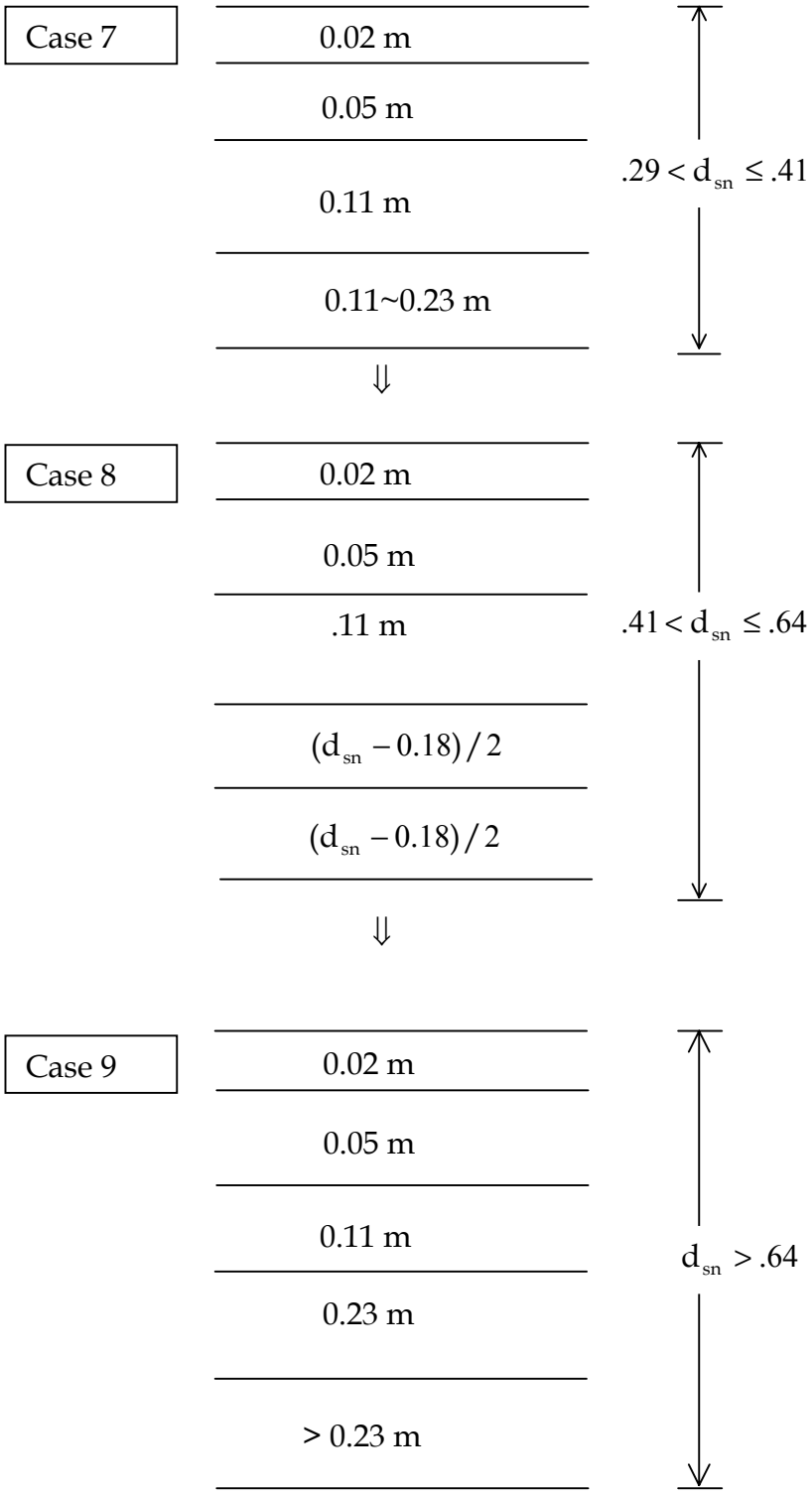

Figure 5.1: Schematic diagram of the finite-difference of snow cover.

6. Surface Albedo and Radiative Fluxes

6.1 *Fraction of snow cover*

The calculation of energy fluxes and albedo will be affected by a treatment of nonuniform snow cover. The current treatment has not undergone any further development but is directly adopted from BATS. Possible improvements in the snow masking rules of BATS have been given in Yang et al (1997). The fraction of soil surface covered by snow S_{cv} is inferred according to the formula:

$$S_{cv} = \frac{\text{snow depth (m)}}{10z_{0g} + \text{ snow depth (m)}} \tag{6.1}$$

where $z_{0g} = 0.01$ (m) is the roughness length for bare soil, *snow depth* is referred to snow water equivalent. The fraction of vegetation buried by snow F_{sn} is given by:

$$F_{sn} = \frac{\text{snow depth (m)}}{10z_{0v} + \text{snow depth (m)}} \tag{6.2}$$

where z_{0v} (m) is the roughness of vegetation. The fraction of vegetation excluding the part buried by snow σ_f is, therefore, given by:

$$\sigma_f = (1 - F_{sn})F_{veg} \tag{6.3}$$

where F_{veg} is the fraction of vegetation in the absence of snow masking.

6.2 *Albedo for snow*

The current treatment of snow albedo has not undergone any further development but is directly adopted from BATS. Further examination is needed of its performance versus the treatment in LSM (Bonan, 1996). The formulae are given by:

$$\alpha_{v,b(snow)} = \alpha_{vd} + 0.4f(\mu)[1 - \alpha_{vd}], \tag{6.4a}$$

$$\alpha_{ir,b(snow)} = \alpha_{ird} + 0.4f(\mu)[1 - \alpha_{ird}], \tag{6.4b}$$

the subscript v refers to visible, ir to near-infrared, b to direct beam, and d denotes diffuse albedos as given by

$$\alpha_{vd} = [1 - 0.2F_{AGE}]\alpha_{vo}$$

$$\alpha_{ird} = [1 - 0.5F_{AGE}]\alpha_{iro}$$

and

α_{vo} = 0.95, the albedo for visible radiation incident on new snow with solar zenith angle less than 60^o

α_{iro} = 0.65, the albedo of new snow for near-infrared solar with solar zenith angle less than 60^o

μ cosine of the solar zenith angle

F_{AGE} a transformed snow age define below and used in this section to give the fractional reduction of snow albedo due to snow aging (assumed to represent increasing grain size and soot) for solar zenith angle less than 60^o

$f(\mu)$ factor between 0 and 1 giving increase of snow visible albedo due to solar zenith angle exceeding 60^o and

$$f(\mu) = \begin{cases} \frac{1}{b}\left[\frac{b+1}{1+2b\mu} - 1\right], & \text{if } \mu \le 0.5 \\ 0, & \text{if } \mu > 0.5 \end{cases} \tag{6.5}$$

where $b = 2.0$, a tunable parameter to help control albedo zenith dependence.

Since snow albedo decreases with time due to growth of snow grain size and accumulation of dirt and soot. F_{AGE} is parameterized as

$$F_{AGE} = \frac{\tau_{snow}}{1+\tau_{snow}} \tag{6.6}$$

where $\tau_{snow} = 0$, if snow water equivalent > 800 (mm), (primarily over Antarctica), otherwise, the nondimensional age of snow τ_{snow} is incremented as a model prognostic variable as follows:

$$\Delta\tau_{snow} = 1\times10^{-6}(r_1 + r_2 + r_3)\Delta t$$

The term r_1 represents the effect of grain growth due to vapor diffusion, the temperature dependence being essentially proportional to the vapor pressure of water:

$$r_1 = \exp\left[5000\left(\frac{1}{T_f} - \frac{1}{T_{snl+1}}\right)\right]$$

The term r_2 represents the additional effect near and at freezing of melt water:

$$r_2 = \min[r_1^{10}, 1]$$

The term r_3 represents the effect of dirt and soot:

$$r_3 = 0.3$$

A snowfall of 0.01 m liquid water is assumed to restore the surface age, hence albedo, to that of new snow. Since the precipitation in model time step will generally be less than that required to so restore the surface when it snows for a given time step, we reduce the snow age by a factor depending on the amount of the fresh snow, as follows:

$$\tau_{snow}^{t+\Delta t} = (\tau_{snow}^{t} + \Delta\tau_{snow})\times[1 - 0.1\max(0, \Delta P_s)] \ge 0$$

where

$$\Delta P_s = [SWE(t+\Delta t) - SWE(t)] \text{ (mm)}$$

Note: the difference of snow albedo for direct and diffuse incident radiation is assumed to be negligible.

6.3 *Albedo for bare soil*

The current treatment has not undergone any further development but is directly adopted from BATS. The albedo for bare soil $\alpha_{\Lambda,\mu}$ are given by

$$\alpha_{v,b(soil)} = \alpha_{sat} + \min[\Delta\alpha_g(\theta_{l,1}), \alpha_{sat}] \tag{6.7a}$$

$$\alpha_{ir,b(soil)} = 2\times\alpha_{v,b(soil)} \tag{6.7b}$$

where α_{sat} is the albedo for a saturated soil (the value for eight color classes used are shown in Table 3) and where the increase of albedo due to dryness of surface soil is given for $\lambda < 0.7$ μm as a function of the ratio of surface soil water volumetric content $\theta_{1,1}$,

$$\Delta\alpha_g(\theta_{1,1}) = \max[0.01\times(11-40\,\theta_{1,1}), 0]$$

Note: the difference of soil albedo for direct and diffuse incident radiation is assumed to be negligible.

6.4 *Albedo for vegetation*

The treatment of canopy albedo has been developed to capture the essential features of a two-stream approximation model while forgoing the complexity of the full treatment. It combines soil and canopy albedo by simple rules that are formulated to reduce to correct asymptotic limits for thick and thin canopies and provide reasonable results for intermediate values of leaf area index. The treatment of canopy radiation to determine PAR in the next section, following LSM, is somewhat different.

(a) The direct beam portion of the reflectance from a finite depth canopy:

$$\alpha_{\Lambda,b(c)} = \alpha_{\Lambda,b(f)}\left[1-\exp\left(-\frac{\omega\beta\,L_{SAI}}{\mu\alpha_{\Lambda,b(f)}}\right)\right] + \alpha_{\Lambda,b(g)}\exp\left[-\left(1+\frac{0.5}{\mu}\right)L_{SAI}\right] \qquad (6.8)$$

The asymptotic behavior of this equation is

$\alpha_{\Lambda,b(c)} \to \alpha_{\Lambda,b(f)}$, as $L_{SAI} \to \infty$, and

$\alpha_{\Lambda,b(c)} \to \alpha_{\Lambda,b(g)} + \omega\beta L_{SAI}/\mu$, as $L_{SAI} \to 0$ (single scattering thin canopy limit).

The above Λ refers to either visible or near-infrared, μ as a subscript either to direct beam (b) or diffuse (d), μ as a variable is the cosine of solar zenith angle, $\alpha_{\Lambda,\mu(f)}$ is the albedo of thick canopy (also called infinite canopy albedo, values of which are listed in Table 2.3 for IGBP land cover types), $\omega\beta$ is the upward scattered fraction (in current version, we simply set $\omega = 0.85$ and $\beta = 0.5$), $\alpha_{\Lambda,\mu(g)}$ is the ground surface albedo.

The above parameterization neglects multiple reflections between canopy and the underlying ground surface. In eq. (6.8), the first term is the albedo for an underlying surface that is black and the second term allows for ground reflection. In principle the exponentials in both terms should be the product of the direct beam transmission and the reflected diffuse beam, corresponding to the second exponential; however, that does not give the right limit for thin canopy. Since $\omega\beta/\alpha_{\Lambda,b(f)}$ is numerically generally close to two, and μ on average about 0.5, the first exponential will usually not differ much from the second. However, its dependence on solar zenith angle is probably only to be trusted in the thin canopy limit. Taking $1-\alpha_{\Lambda,b(c)}$ gives the total energy absorbed by canopy and ground. That absorbed by the canopy is then obtained by subtracting that absorbed by the ground, i.e., the ground absorption reduced by canopy direct beam attenuation. The fraction of the direct beam absorbed by canopy is given by

$$F_{\Lambda,b(c)} = 1 - \alpha_{\Lambda,b(c)} - (1 - \alpha_{\Lambda,b(g)}) \exp\left(- \frac{0.5 L_{SAI}}{\mu} \right) \tag{6.9}$$

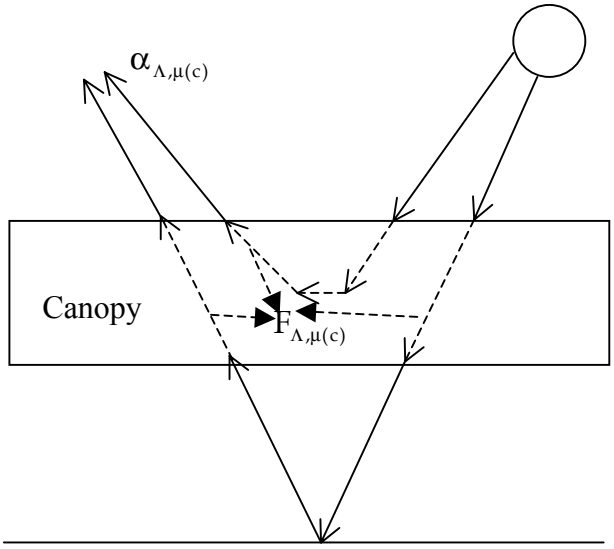

Figure 6.1. Schematic representation of the direct and diffuse solar components considered in this albedo scheme. Canopy attenuation: $\exp[-0.5 L_{SAI} / \mu]$ for direct beam, $\exp(-L_{SAI})$ for diffuse beam.

(b) The diffusive portion of the reflectance from a finite depth canopy:
It can be obtained from (6.8) with μ = 0.5, i.e.,

$$\alpha_{\Lambda,d(c)} = \alpha_{\Lambda,d(f)} \left[1 - \exp\left(- \frac{2\omega\beta L_{SAI}}{\alpha_{\Lambda,d(f)}} \right) \right] + \alpha_{\Lambda,d(g)} \exp[-2 L_{SAI}] \tag{6.10}$$

The fraction of the diffusive solar absorbed by canopy $F_{\Lambda,d(c)}$ is,

$$F_{\Lambda,d(c)} = 1 - \alpha_{\Lambda,d(c)} - (1 - \alpha_{\Lambda,d(g)}) \exp(-L_{SAI}) \tag{6.11}$$

6.5 *Averaged surface albedo*

Effective albedo over vegetation with snow

$$\bar{\alpha}_{\Lambda,\mu(c)} = (1 - F_{sn})\, \alpha_{\Lambda,\mu(c)} + F_{sn} \alpha_{\Lambda,\mu(snow)} \tag{6.12}$$

Effective albedo over bare soil covered by snow

$$\bar{\alpha}_{\Lambda,\mu(g)} = (1 - S_{cv})\, \alpha_{\Lambda,\mu(soil)} + S_{cv} \alpha_{\Lambda,\mu(snow)} \tag{6.13}$$

Weighted albedo over grid

$$\bar{\alpha}_{\Lambda,\mu} = (1 - F_{veg})\, \bar{\alpha}_{\Lambda,\mu(g)} + F_{veg}\, \bar{\alpha}_{\Lambda,\mu(c)} \tag{6.14}$$

6.6 *Radiation absorbed by canopy and ground*

(a) Solar fluxes

Net solar absorbed by surface (total),

$$S_n = \sum_{\Lambda,\mu} (1 - \bar{\alpha}_{\Lambda,\mu}) S^{\downarrow}_{\Lambda,\mu} \tag{6.15}$$

Net solar absorbed by canopy,

$$S_{n,c} = \sigma_f \sum_{\Lambda,\mu} F_{\Lambda,\mu(c)} S^{\downarrow}_{\Lambda,\mu} \tag{6.16}$$

where σ_f is the snow-free vegetation fraction as defined in eq. (6.3).

Net solar absorbed by ground,

$$S_{n,g} = S_n - S_{n,c} \tag{6.17}$$

(b) Long-wave fluxes

(add a schematic figure as Figure 12 in LSM page 40 ?)

Net longwave radiation absorbed by canopy,

$$L_{n,c} = a + bT_c^4 + cT_g^4 \tag{6.18}$$

$$a = \sigma_f \varepsilon_v [1 + (1 - \varepsilon_v)(1 - \varepsilon_g)] L^{\downarrow}_a$$

$$b = -\sigma_f \sigma \varepsilon_v [2 - \varepsilon_v (1 - \varepsilon_g)]$$

$$c = \sigma_f \sigma \varepsilon_v \varepsilon_g$$

where $L^{\downarrow}_a$ is the downward atmospheric longwave radiation, σ is the Stefan-Boltzmann constant. Net longwave absorbed by ground,

$$L_{n,g} = a + bT_c^4 + cT_g^4 \tag{6.19}$$

$$a = \varepsilon_g [(1 - \sigma_f) + \sigma_f (1 - \varepsilon_v)] L^{\downarrow}_a$$

$$b = \sigma_f \sigma \varepsilon_v \varepsilon_g$$

$$c = -\sigma \varepsilon_g$$

The emissivity of ground is $\varepsilon_g = 0.97$ for snow accumulation (or glaciers) case, $\varepsilon_g = 0.96$ for bare ground (or wetland) case. The vegetation emissivity is $\varepsilon_v = 1 - \exp(-L_{SAI})$. The above equations allow for the emissivities less than one, and assume absorptivity equals emissivity. The term $1 - \varepsilon_v$ is the transmitted fraction through the canopy, and $1 - \varepsilon_g$ is the fraction reflected by ground.

The radiative temperature (skin temperature) of surface is as an important diagnostic variable in climate modeling and remote sensing analysis, and defined from the outgoing longwave flux from surface,

$$T_{rad} = (L^{\uparrow} / \sigma)^{1/4} \tag{6.20}$$

$$L^{\uparrow} = \sigma_f (1 - \varepsilon_v)[(1 - \varepsilon_g)(1 - \varepsilon_v) L^{\downarrow}_a + \varepsilon_v (1 - \varepsilon_g) \sigma T_c^4 + + \varepsilon_g \sigma T_g^4] + \sigma_f \varepsilon_v \sigma T_c^4$$

$$+ (1 - \sigma_f)[(1 - \varepsilon_g) L^{\downarrow}_a + \varepsilon_g \sigma T_g^4].$$

7. Stomatal Resistance

The current submodel of stomatal resistance has not undergone any further development but is directly adopted from LSM (Bonan, 1996).

7.1 *Photosynthetically Active Radiation Absorbed by the Canopy*

Photosynthesis and transpiration depend non-linearly on solar radiation, via the light response of stomata. A common way to integrate CO_2 and H_2O fluxes for the canopy is to divide the canopy into sunlit and shaded leaves (Campbell 1977, Landsberg 1986). The sunlit fraction of the canopy is

$$f_{sun} = \frac{1}{L_{AI}} \int_0^{L_{AI}} e^{-k_b x} dx = \frac{1}{k_b L_{AI}} (1 - e^{-k_b L_{AI}}) \tag{7.1a}$$

where L_{AI} is the leaf area index, in which the stem area index (S_{AI}) is not included as LSM (Bonan 1996); k_b is the PAR extinction coefficient for direct beam solar (time-mean radiation-weighted value), and $k_b = \frac{G(\mu)}{\mu}\sqrt{1-\omega_v}$; $G(\mu)$ is the projection of leaves in the direction of the incoming radiation flux, currently, a random distribution for leaves is assumed, i.e., $G(\mu) = 0.5$; μ is cosine of the solar zenith angle; ω_v is the leaf-scattering coefficient (single scattering reflectance) for PAR, for simplicity, $\omega_v = 0.15$ is assumed. To prevent numerical instabilities, set f_{sun} to 0 when the sunlit fraction is less than 1%. The shaded fraction of the canopy is

$$f_{sha} = 1 - f_{sun} \tag{7.1b}$$

and the sunlit and shaded leaf area indices are

$$L_{sun} = f_{sun} L_{AI} \tag{7.2a}$$

$$L_{sha} = f_{sha} L_{AI} \tag{7.2b}$$

The solar radiation absorbed by the vegetation in the visible waveband (< 0.7 μm) is partitioned to sunlit and shaded leaves to calculate the average absorbed photosynthetically active radiation for sunlit and shaded leaves. For $f_{sun} > 0$

$$\phi_{sun} = (I_b + f_{sun} I_d) \frac{1}{L_{sun}} \tag{7.3a}$$

$$\phi_{sha} = f_{sha} I_d \frac{1}{L_{sha}} \tag{7.3b}$$

where I_b is the direct beam solar radiation (visible component) absorbed by the canopy,

$$I_b = (1 - \alpha_{v,b(c)}) S^{\downarrow}_{v,b} \times [1 - \exp(-k_b L_{SAI})] \tag{7.4a}$$

and I_d is the diffuse solar radiation (visible) absorbed by the canopy,

$$I_d = (1 - \alpha_{v,d(c)}) S^{\downarrow}_{v,d} \times [1 - \exp(-k_d L_{SAI})] \tag{7.4b}$$

where $k_d = \sqrt{1-\omega_v}$ is the PAR extinction coefficient for diffuse solar radiation (time-mean radiation-weighted value). If $f_{sun} = 0$, all the radiation is absorbed by the shaded leaves. This special condition is needed because $f_{sun} = 0$ if less than 1% of the canopy is

sunlit, in which case direct beam radiation that would otherwise be absorbed by the sunlit canopy needs to be included in the shaded fraction. Note: equations (7.4) are somewhat different from the LSM's definitions.

7.2 *Photosynthesis and Stomatal Resistance*

Leaf stomatal resistance is coupled to leaf photosynthesis in a manner similar to Collatz et al. (1991) (see also Sellers et al. 1992)

$$\frac{1}{r_s} = m\frac{A}{c_s}\frac{e_s}{e_i}p_s + b \tag{7.5}$$

where

r_s Leaf stomatal resistance (s m^2 μ mol^{-1}),
m An empirical parameter (9),
A Leaf photosynthesis (μ mol CO_2 m^{-2} s^{-1}),
c_s CO_2 concentration at the leaf surface (pa),
e_s Vapor pressure at the leaf surface (pa),
e_i Saturation vapor pressure (pa) inside the leaf at the vegetation temperature,
p_s Atmospheric pressure at surface (pa),
b Minimum stomatal conductance (2000 μ mol m^{-2} s^{-1}) when $A = 0$.

Leaf photosynthesis is $A = \min(w_c, w_j, w_e)$. $A = 0$ when the vegetation temperature $T_v \le T_{min}$. The C_4 feature of the model is not currently used since the IGBP land cover types do not distinguish between C_3 and C_4 types. The RuBP carboxylase (Rubisco) limited rate of carboxylation is

$$w_c = \frac{(c_i - \Gamma_*)V_{max}}{c_i + K_c(1 + o_i / K_o)} \tag{7.6}$$

The maximum rate of carboxylation allowed by the capacity to regenerate RuBP (i.e., the light limited rate) is

$$w_j = \frac{(c_i - \Gamma_*)4.6\phi\alpha}{c_i + 2\Gamma_*} \tag{7.7}$$

The export limited rate of carboxylation for C_3 plants and the PEP carboxylase limited rate of carboxylation for C_4 plants is

$$w_e = 0.5V_{max} \tag{7.8}$$

In above equations, c_i is the internal CO_2 concentration (Pa); o_i is O_2 concentration (Pa), and $o_i = 0.209p_s$; K_c and K_o are Michaelis-Menten constants (Pa) for CO_2 and O_2, respectively, which vary with vegetation temperature T_v (ºC) = $T_c - T_f$, $K_c = K_{c25}a_{kc}^{(T_v-25)/10}$ and $K_o = K_{o25}a_{ko}^{(T_v-25)/10}$, where K_{c25} and K_{o25} are the values at 25ºC and a_{kc} and a_{ko} are temperature sensitivity parameters; $\Gamma_* = \frac{1}{2}\frac{K_c}{K_0}0.21o_i$ is the CO_2 compensation point (pa), the term 0.21 represents the ratio of maximum rates of oxygenation to carboxylation, which is virtually constant with temperature; α is the

quantum efficiency; ϕ is the absorbed photosynthetically active radiation (W m^{-2}) (section 7.1), which is converted to photosynthetic photon flux assuming 4.6 μmol photons per Joule.

The maximum rate of carboxylation varies with temperature, foliage nitrogen, and soil water

$$V_{max} = V_{max25} a_{vmax}^{\frac{T_v - 25}{10}} f(N) f(T_v) f(w) \tag{7.9}$$

where V_{max25} is the value at 25ºC and a_{vmax} is a temperature sensitivity parameter. $f(T_v)$ is a function that mimics thermal breakdown of metabolic processes

$$f(T_v) = \left[1 + \exp\left(\frac{-220000 + 710(T_v + 273.16)}{8.314(T_v + 273.16)} \right) \right]^{-1} \tag{7.10}$$

$f(N) = N / N_{max} \le 1$ adjusts the rate of photosynthesis for foliage nitrogen N. Currently, $f(N) = 1$ so that values of V_{max25} already include nitrogen limitation. $f(w)$ is a function that decreases photosynthesis and increases stomatal resistance as the soil dries. Currently, $f(w) = 1$. Soil water limitations on photosynthesis and transpiration are accounted for by limiting the transpiration to the maximum that can be sustained by the vegetation (section 3.7).

The CO_2 concentration at the leaf surface c_s (pa), the internal leaf CO_2 concentration c_i (pa), and the vapor pressure at the leaf surface e_s (pa) are calculated assuming there is negligible capacity to store CO_2 and water vapor at the leaf surface so that

$$A = \frac{c_a - c_i}{(1.37 r_b + 1.65 r_s) p_s} = \frac{c_a - c_s}{1.37 r_b p_s} = \frac{c_s - c_i}{1.65 r_s p_s} \tag{7.11}$$

and the transpiration fluxes are related as

$$\frac{e'_a - e_i}{(r_b + r_s)} = \frac{e'_a - e_s}{r_b} = \frac{e_s - e_i}{r_s} \tag{7.12}$$

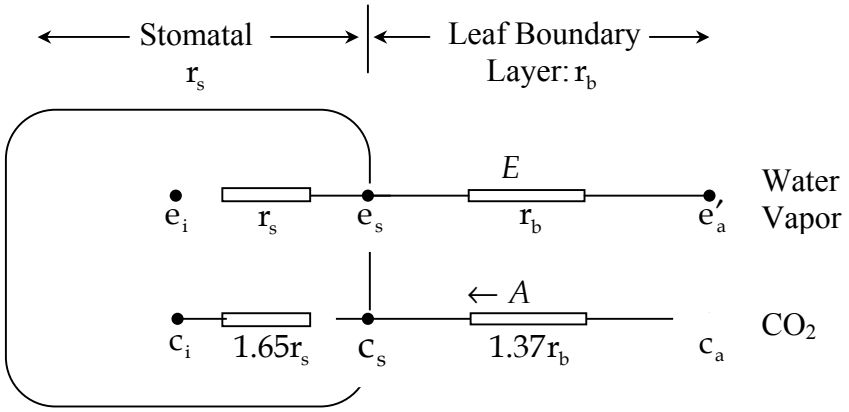

Figure 7.1. Schematic diagram of the leaf stomatal photosynthesis-condutance model. System shows for water vapor and CO_2 flux. The term r_b refers to the leaf laminar boundary-layer resistance for vapor flux, r_s refers to the stomatal resistance.

where

r_b Leaf boundary layer resistance (s m^2 μmol^{-1}) (section 4.2), the terms 1.37 and 1.65 are the ratios of diffusivity of CO_2-to-H_2O for the leaf boundary layer resistance and stomatal resistance,

c_a Atmospheric CO_2 concentration (pa), and $c_a = 355 \times 10^{-6} p_s$,

e'_a Vapor pressure of air (pa), and $e'_a = \max[0.25e_i, \min(e_a, e_i)]$, the lower limit $0.25e_i$ is used to prevent numerical instability in the iterative stomatal resistance calculation,

e_a Vapor pressure of air in the plant canopy, which was described in section 4.2.

With $c_s = \max(c_a - 1.37 r_b P_s A,\ 10^{-6})$ and $e_s = \dfrac{e'_a r_s + e_i r_b}{r_b + r_s}$, stomatal resistance is the larger of two roots that satisfy the quadratic equation

$$\left(\frac{mAp_s e'_a}{c_s e_i} + b\right) r_s^2 + \left(\frac{mAp_s r_b}{c_s} + br_b - 1\right) r_s - r_b = 0 . \qquad (7.13)$$

This equation is iterated three times with an initial arbitrary value of $c_i = 0.7 c_a$ used to calculate A. Subsequent values for c_i are given by $c_i = \max(c_s - 1.65 r_s p_s A,\ 0)$.

These equations are solved for sunlit and shaded leaves using average absorbed photosynthetically active radiation for sunlit and shaded leaves (ϕ_{sun}, ϕ_{sha} [section 7.1]) to give sunlit and shaded stomatal resistance ($r_{s,sun}$, $r_{s,sha}$) and photosynthesis (A_{sun}, A_{sha}). Canopy photosynthesis is $A_{sun} L_{sun} + A_{sha} L_{sha}$, where L_{sun} and L_{sha} are the sunlit and shaded leaf area indices (section 7.1). Canopy conductance is $L_{sun} / r_{s,sun} + L_{sha} / r_{s,sha}$. The canopy integration technique used here allows both sunlit and shaded leaves to photosynthesize, although at different rates depending on the amount of absorbed photosynthetically active radiation.

Photosynthetic parameters are listed in Table 5 for each IGBP land cover type. Note that the parameters are currently specified identically for all IGBP land cover types. K_{c25}, K_{o25}, a_{kc}, a_{ko}, a_{vmax} and m are from Collatz et al. (1991). α is based on typical values given in Landsberg (1986). b was chosen to give a maximum stomatal resistance of 20000 s m^{-1}. T_{min} is a typical value of when plants photosynthesize with respect to temperature. V_{max25} was chosen to give a maximum photosynthetic rate of 10 μmol CO_2 m^{-2} s^{-1}.

8. Turbulent Fluxes

8.1 *Roughness lengths and zero-plane displacement*

Aerodynamic roughness z_{0m} is used for wind, while thermal roughness z_{0h} is used for heat and water vapor. In general, z_{0m} is different from z_{0h}, because the transfer of momentum is affected by pressure fluctuations in the turbulent waves behind the roughness elements, whilst for heat and water vapor transfer no such dynamical mechanism exists. Rather, heat and water vapor must ultimately be transferred by molecular diffusion across the interfacial sublayer. Over bare soil and snow cover, the simple relation from Zilitinkevich (1970) can be used (Zeng and Dickinson 1998):

$$\ln\frac{z_{0m}}{z_{0h}} = a\left(\frac{u_* z_{0m}}{\nu}\right)^{0.45}, \quad a = 0.13, \quad \nu = 1.5\times10^{-5}\,m^2 s^{-1} \tag{8.1}$$

Over canopy, the use of energy balance (see eq.4.21) is equivalent to the use of different z_{0m} versus z_{0h} over bare soil, and hence thermal roughness is not needed over canopy (Zeng et al. 1998).

The roughness z_{0m} is proportional to canopy height, and is also affected by fractional vegetation cover, leaf area index, and leaf shapes. When canopy height (h_c) cannot be accurately determined, the simple relationship $z_{0m} = 0.07h_c$ can be used.

Similarly, the zero-plane displacement height d is proportional to canopy height, and is also affected by fractional vegetation cover, leaf area index, and leaf shapes. When canopy height (h_c) cannot be accurately determined, the simple relationship $d/h_c = 2/3$ can be used.

8.2 *Monin-Obukhov similarity theory*

(1) Turbulence scaling parameters

A length scale (the Monin-Obukhov length) L is defined by

$$L = \frac{\theta_v u_*^2}{kg\theta_{v*}} \tag{8.2}$$

where k is the von Kárman constant, g is the gravitational acceleration. $L > 0$ indicates stable conditions, $L < 0$ indicates unstable conditions, $L = \infty$ for neutral conditions. The virtual potential temperature θ_v is defined by

$$\theta_v = \theta_a(1+0.61q_a) = T_a\left(\frac{p_s}{p_l}\right)^{R/c_p}(1+0.61q_a) \tag{8.3}$$

where T_a and q_a are the air temperature and specific humidity at height z_r respectively, θ_a is the atmospheric potential temperature, p_l is the atmospheric pressure, p_s is the surface pressure. The surface friction velocity u_* is defined by

$$u_*^2 = [\overline{u'w'}^2 + \overline{v'w'}^2]^{1/2} \tag{8.4}$$

Temperature scale θ_* and θ_{*v} and a humidity scale q_* are defined by

$$\theta_* = -\overline{w'\theta'}/u_* \tag{8.5}$$

$$q_* = -\overline{w'q'}/u_* \tag{8.6}$$

$$\theta_{v*} = -\overline{w'\theta'_v}/u_* \approx -(\overline{w'\theta'} + 0.61\bar{\theta}\overline{w'q'})/u_* = \theta_* + 0.61\bar{\theta}q_* \tag{8.7}$$

(where the mean temperature $\bar{\theta}$ serves as a reference temperature in this linearized form of θ_v).

The stability parameter is defined as

$$\varsigma = \frac{z_r - d}{L}, \text{ with the restriction: } -100 \le \varsigma \le 2 \tag{8.8}$$

The scalar wind speed is defined as

$$V_a^2 = u_a^2 + v_a^2 + U_c^2 \tag{8.9}$$

$$U_c = \begin{cases} 0.1 \text{ ms}^{-1}, \text{if } \varsigma \ge 0 \quad \text{(stable)} \\ \beta w_* = \beta\left(z_i \dfrac{g}{\theta_v}\theta_{v*}u_*\right)^{1/3}, \text{ if } \varsigma < 0 \quad \text{(unstable)} \end{cases} \tag{8.10}$$

w_* is the convective velocity scale, z_i is the convective boundary layer height, the value of z_i is taken as 1000 m, and $\beta = 1$.

(2) Flux-gradient relations (Zeng et al. 1998)

(8.11)

$$\frac{k(z_r - d)}{\theta_*}\frac{\partial\theta}{\partial z} = \phi_h(\varsigma) \tag{8.12}$$

$$\frac{k(z_r - d)}{q_*}\frac{\partial q}{\partial z} = \phi_q(\varsigma) \tag{8.13}$$

where

$$\left.\begin{aligned} &\phi_h = \phi_q \\ &\phi_m(\varsigma) = (1 - 16\varsigma)^{-1/4} \\ &\phi_h(\varsigma) = (1 - 16\varsigma)^{-1/2} \end{aligned}\right\}, \quad \text{for } \varsigma < 0$$

$$\phi_m(\varsigma) = \phi_h(\varsigma) = 1 + 5\varsigma, \quad \text{for } 0 < \varsigma < 1$$

Under very unstable conditions, the flux-gradient relations from Kader and Yaglom (1990) are used,

$$\phi_m = 0.7k^{2/3}(-\varsigma)^{1/3}, \text{ and } \phi_h = 0.9k^{4/3}(-\varsigma)^{-1/3}$$

To ensure continuous function of $\phi_m(\varsigma)$ and $\phi_h(\varsigma)$, the simplest approach (i.e., without considering any transition regions) is to match the above equations at $\varsigma_m = -1.574$ for $\phi_m(\varsigma)$ and $\varsigma_h = -0.465$ for $\phi_h(\varsigma)$.

Under very stable conditions (i.e., $L > 1$), relations from Holtslag et al. (1990) can be used,

$$\phi_m = \phi_h = 5 + \varsigma$$

(3) Integral forms of the flux-gradient relations
Integration of wind profile,

$$V_a = \frac{u_*}{k} f_M(\varsigma) \tag{8.14}$$

$$f_M(\varsigma) = \left\{ \left[\ln\left(\frac{\varsigma_m L}{z_{0m}}\right) - \psi_m(\varsigma_m) \right] + 1.14[(-\varsigma)^{1/3} - (-\varsigma_m)^{1/3}] \right\} \tag{8.14a}$$

for $\varsigma < \varsigma_m = -1.574$

$$f_M(\varsigma) = \left[\ln\left(\frac{z_r - d}{z_{0m}}\right) - \psi_m(\varsigma) + \psi_m\left(\frac{z_{0m}}{L}\right) \right] \tag{8.14b}$$

for $\varsigma_m < \varsigma < 0$

$$f_M(\varsigma) = \left[\ln\left(\frac{z_r - d}{z_{0m}}\right) + 5\varsigma \right] \tag{8.14c}$$

for $0 < \varsigma < 1$

$$f_M(\varsigma) = \left\{ \left[\ln\left(\frac{L}{z_{0m}}\right) + 5 \right] + [5\ln(\varsigma) + \varsigma - 1] \right\} \tag{8.14d}$$

for $\varsigma > 1$

Integration of potential temperature profile,

$$\theta_a - \theta_s = \frac{\theta_*}{k} f_T(\varsigma) \tag{8.15}$$

$$f_T(\varsigma) = \left\{ \left[\ln\left(\frac{\varsigma_h L}{z_{0h}}\right) - \psi_h(\varsigma_h) \right] + 0.8\,[(-\varsigma_h)^{-1/3} - (-\varsigma)^{-1/3}] \right\} \tag{8.15a}$$

for $\varsigma < \varsigma_h = -0.465$

$$f_T(\varsigma) = \left[\ln\left(\frac{z_r - d}{z_{0h}}\right) - \psi_h(\varsigma) + \psi_h\left(\frac{z_{0h}}{L}\right) \right], \text{ for } \varsigma_h < \varsigma < 0 \tag{8.15b}$$

$$f_T(\varsigma) = \left[\ln\left(\frac{z_r - d}{z_{0h}}\right) + 5\varsigma \right], \text{ for } 0 < \varsigma < 1 \tag{8.15c}$$

$$f_T(\varsigma) = \left\{ \left[\ln\left(\frac{L}{z_{0h}}\right) + 5 \right] + [5\ln(\varsigma) + \varsigma - 1] \right\}, \text{ for } \varsigma > 1 \tag{8.15d}$$

The integration of specific humidity profiles is the same as those for potential temperature except that $(\theta_a - \theta_s)$, θ_* and z_{0h} are replaced by $(q_a - q_s)$, q_* and z_{0q} respectively. The stability functions are

$$\left.\begin{aligned}\psi_m &= 2\ln\left(\frac{1+\chi}{2}\right) + \ln\left(\frac{1+\chi^2}{2}\right) - 2\tan^{-1}\chi + \frac{\pi}{2}\\ \psi_h &= \psi_q = 2\ln\left(\frac{1+\chi^2}{2}\right)\end{aligned}\right\},\quad \varsigma < 0$$

$$\chi = (1-16\varsigma)^{1/4}$$

For vegetation, $\theta_s = T_{af}$, $q_s = q_{af}$; for bare soil, $\theta_s = T_g$, $q_s = q_g$.

Note that the CLM code contains extra terms involving z_{0m}/ς, z_{0h}/ς, and z_{0q}/ς for completeness. These terms are very small most of the time and hence are omitted in Eqs. (8.14) and (8.15).

8.3 *Fluxes*

The momentum, sensible heat and water vapor fluxes between the surface and the reference height z_r can be written in the form,

$$\tau_x = -\rho_a\overline{(u'w')} = -\rho_a u_*^2(u_a/V_a) = -\rho_a\frac{u_a}{r_{am}} \tag{8.16a}$$

$$\tau_y = -\rho_a\overline{(v'w')} = -\rho_a u_*^2(v_a/V_a) = -\rho_a\frac{v_a}{r_{am}} \tag{8.16b}$$

$$H = \rho_a c_p(\overline{w'\theta'}) = -\rho_a c_p u_*\theta_* = \rho_a c_p\frac{\theta_s - \theta_a}{r_{ah}} \tag{8.17}$$

$$E = \rho_a(\overline{w'q'}) = -\rho_a u_* q_* = \rho_a\frac{q_s - q_a}{r_{aw}} \tag{8.18}$$

$$r_{am} = V_a/u_*^2 \tag{8.19}$$

$$r_{ah} = (\theta_a - \theta_s)/u_*\theta_* \tag{8.20}$$

$$r_{aw} = (q_a - q_s)/u_* q_* \tag{8.21}$$

A 2-meter height "screen" temperature is an important diagnostic variable in climate modelling, which was widely provided by the routine meteorological measurement, and given by:

$$T_{2m} - \theta_a = \frac{\theta_*}{k}\left[f_T\left(\frac{z_{0h}+2}{L}\right) - f_T\left(\frac{z_r - d}{L}\right)\right] \tag{8.22}$$

where "2 m" is defined as 2 m above the apparent sink for sensible heat. For non-vegetated part of cell, T_s is the ground surface temperature, z_{0h} refers to the value of ground. For vegetated part, T_s is the canopy air temperature, z_{0h} refers to the value of vegetation.

Appendix 1: Physical Constants

Table A1. Physical Constants

	Definition	Value	Unit
ρ_i	Density of ice	917.	kg m^{-3}
ρ_l	Density of liquid water	1000.	kg m^{-3}
c_l	Specific heat of water	4217.7	J $kg^{-1}K^{-1}$
c_i	Specific heat of ice	2117.27	J $kg^{-1}K^{-1}$
c_p	Specific heat of dry air	1004.67	J $kg^{-1}K^{-1}$
L_f	Latent heat of fusion for ice	0.3336×10^{6}	J kg^{-1}
L_v	Latent heat of evaporation for water	2.5104×10^{6}	J kg^{-1}
L_s	Latent heat of sublimation	2.8440×10^{6}	J kg^{-1}
λ_a	Thermal conductivity of air	0.023	W $m^{-1}K^{-1}$
λ_i	Thermal conductivity of ice	2.290	W $m^{-1}K^{-1}$
λ_w	Thermal conductivity of water	0.6	W $m^{-1}K^{-1}$
T_f	Freezing temperature	273.16	K
R	Gas constant for dry air	287.1	J $kg^{-1}K^{-1}$
R_w	Gas constant for water vapor	461.296	J $kg^{-1}K^{-1}$
b	Gravity constant	9.80616	m s^{-2}
k	von Kárman constant	0.4	-
σ	Stefan-Boltzmann constant	5.67×10^{-8}	W $m^{-2}K^{-4}$

Appendix 2: Saturation Vapor Pressure (SVP)

Saturation vapor $e_{sat}(T)$ as a function of temperature T (^oC) and $de_{sat}(T)/dT$ are calculated using a polynomial fits (Flatau et al. 1992) as:

$$e_{sat}(T) = 100\,[a_0 + a_1(T - T_f) + \cdots + a_n(T - T_f)^n]$$

$$de_{sat}(T)/dT = 100\,[b_0 + b_1(T - T_f) + \cdots + b_n(T - T_f)^n]$$

Here the T_f is equal to 273.15 K.

Table A2. Coefficients of the eight-order polynomial fits to SVP and its temperature derivative over water for temperature range 0^o – 100^oC. Same for ice but for the range – 75^o – 0^oC.

Coefficients	Water vapor (0^o – 100^oC)	Ice (-75^o – 0^oC)
A_0	6.11213476	6.11123516
A_1	0.444007856	0.503109514
A_2	$0.143064234\times10^{-01}$	$0.188369801\times10^{-01}$
A_3	$0.264461437\times10^{-03}$	$0.420547422\times10^{-03}$
A_4	$0.305903558\times10^{-05}$	$0.614396778\times10^{-05}$
A_5	$0.196237241\times10^{-07}$	$0.602780717\times10^{-07}$
A_6	$0.892344772\times10^{-10}$	$0.387940929\times10^{-09}$
A_7	$-0.373208410\times10^{-12}$	$0.149436277\times10^{-11}$
A_8	$0.209339997\times10^{-15}$	$0.262655803\times10^{-14}$
Derivative		
B_0	0.444017302	0.503277922
B_1	$0.286064092\times10^{-01}$	$0.377289173\times10^{-01}$
B_2	$0.794683137\times10^{-03}$	$0.126801703\times10^{-02}$
B_3	$0.121211669\times10^{-04}$	$0.249468427\times10^{-04}$
B_4	$0.103354611\times10^{-06}$	$0.313703411\times10^{-06}$
B_5	$0.404125005\times10^{-09}$	$0.257180651\times10^{-08}$
B_6	$-0.788037859\times10^{-12}$	$0.133268878\times10^{-10}$
B_7	$-0.114596802\times10^{-13}$	$0.394116744\times10^{-13}$
B_8	$0.381294516\times10^{-16}$	$0.498070196\times10^{-16}$

Saturated water-vapor specific humidity:

$$q_{sat}(T) = \frac{0.622\,e_{sat}(T)}{p - 0.378\,e_{sat}(T)}$$

Derivative of the saturated water-vapor specific humidity:

$$\frac{dq_{sat}(T)}{dT} = \frac{0.622p}{[p - 0.378\,e_{sat}(T)]^2}\frac{de_{sat}(T)}{dT}$$

Appendix 3: Solar Zenith Angle

The cosine of the solar zenith angle is

$$\mu = \sin\phi\sin\delta + \cos\phi\cos\delta\cos h$$

where ϕ is latitude (positive in the northern hemisphere), δ is the solar declination, and h is the solar hour angle (24 hour periodicity). The solar declination (radians) depends on the calendar day d

$$\delta = 0.006918 - 0.399912\cos\theta + 0.070257\sin\theta$$
$$- 0.006758\cos 2\theta + 0.000907\sin 2\theta$$
$$- 0.002697\cos 3\theta + 0.001480\sin 3\theta$$

where $\theta = 2\pi\frac{d}{365}$. The solar hour angle (radians) is 15^o for every hour from local noon

$$h = 15(t-12)\frac{\pi}{180}$$

The local time t (hours) at longitude θ (radians, positive East of the Greenwich meridian) is obtained by adjusting m, the current seconds in the day at Greenwich, by 1 hour for every 15^o of longitude

$$t = (m + 86400\theta/2\pi)/3600$$

This calculation of μ, which depends on latitude, longitude, and Greenwich time, matches the algorithm used in the NCAR CCM2 to within ± 0.0001.

Appendix 4: IGBP Land Cover Types Definition

The IGBP classification uses no climatic factors in class definition; categories are generally based on the philosophy proposed by Running et al. (1994) but modified to be compatible with classification systems current used for environmental modeling, represent landscape mixtures and mosaics, and where possible, provide land use implications. The classification is based on definitions of three canopy components: above ground biomass, leaf longevity, and leaf type, the detail for each category is shown in Table A3.

Table A3. IGBP Land Surface Classification and Definition

	Natural Vegetation	
1	Evergreen Needleleaf Forest	Land dominated by woody vegetation with a percent cover > 60%; Height exceeding 2 meters; Almost all trees remain green all year. Canopy is never without green foliage.
2	Evergreen Broadleaf Forests	Lands dominated by woody vegetation with a percent cover > 60%; Height exceeding 2 meters; Almost all trees and shrubs remain green year round. Canopy in never without green foliage.
3	Deciduous Needleleaf Forests	Land dominated by woody vegetation with percent cover > 60%; Height exceeding 2 meters; Consists of seasonal needleleaf tree communities with an annual cycle of leaf-on and leaf-off periods.
4	Deciduous Broadleaf Forests	Land dominated by woody vegetation with percent cover > 60%; Height exceeding 2 meters; Consists of broadleaf tree communities with an annual cycle of leaf-on and leaf-off periods.
5	Mixed Forests	Land dominated by woody vegetation with percent cover > 60%; Height exceeding 2 meters; Consists of broadleaf tree communities with an annual cycle of leaf-on and leaf-off periods.
6	Closed Shrublands	Land with shrub canopy cover > 60%; With woody vegetation less than 2 meters tall; The shrub foliage can be either evergreen or deciduous.
7	Open Shrublands	Land with shrub canopy cover between 10 – 60%; With woody vegetation less than 2 meters tall; The shrub foliage can be either evergreen or deciduous.
8	Woody Savannas	Land with forest canopy cover between 30 – 60%; Forest cover height exceeds 2 meters; With herbaceous and other understory systems.

9	Savannas	Land with forest canopy cover between 10 – 30%; Forest cover height exceeds 2 meters; With herbaceous and other understory systems.
10	Grasslands	Tree and shrub cover is less than 10%; With herbaceous types of cover.
11	Permanent Wetlands	Land with a permanent mixture of water and herbaceous or woody vegetation; the vegetation can be present in either salt, brackish, or fresh water.
	Developed and Mosaic Lands	
12	Croplands	Lands covered with temporary crops followed by harvest and bare soil period (e.g., single and multiple cropping systems). Note that perennial woody crops will be classified as the appropriate forest or shrub land cover type
13	Urban and Built-Up Lands	Land covered by buildings and other man-made structures.
14	Cropland / Natural Vegetation Mosaics	Lands with a mosaic of croplands, forests, shrubland, and grasslands in which no one component comprises more than 60% of the landscape.
	Non-Vegetation Lands	
15	Snow and Ice	Lands under snow/ice cover throughout the years.
16	Barren	Lands with exposed soil, sand, rocks, or snow and never has more than vegetated cover during any time of the year.
17	Water Bodies	Oceans, seas, lakes, reservoir, and rivers. Can be either fresh or salt-water bodies
18	Bare Soil	Bare soil throughout the years

Appendix 5. Sequence of calculations of CLM

Model initializations

Ξ Read in the surface data on [lon] × [lat] grid.

Ξ Gathering the "lpt" land points on [lon] × [lat] → [lpt] → big vector of [kpt] points, assign the surface data to 1D vector of [kpt].

Ξ Define the vertical discretization and assign the parameters to each layer. Get the time-invariant data (soil properties, vegetation parameters) based on soil constituent percentage and vegetation types to 1D big vector of [kpt], and the vertical variables with dimension of [snl+1 : msl, kpt].

Ξ Initializations of state variables (read in or arbitrarily assign or base on the observation) to 1D vector of [kpt], and the vertical variables with dimension of [snl+1 : msl, kpt].

Ξ Average the subgrid albedoes, surface temperature, snow water depth, and outgoing longwave, surface temperature, and other land surface variables (e.g.,) required by the atmospheric model. Return these variables to the atmospheric model from [kpt] vector of subgrid points → [lpt] vector of land points → [lon] × [lat] grid.

Time loop

Calculate surface fluxes and update the hydrological, thermal and ecological state of the land. The processing of each land grid point by subroutine "clm_drv" begins by gathering the [lpt] land points on [lon] × [lat] grid into a big vector of [kpt] points, allowing for up to [msub=5] grid points per land point.

1***. Get atmospheric forcings and map atmospheric fields to force clm: [lon] × [lat] grid → [lpt] vector of land points → [kpt] vector of subgrid points. (get_met.f90)

All calculations from 2 –10 are bounded at 1D of [1:kpt]

2. Solar absorbed by vegetation and ground. (surrad.f90)
3. Main driver for CLM (clm_main.f90)

    Ξ Canopy interception and precipitation onto ground surface.
    Ξ Separate snowfall and rainfall at a critical air temperature; get the density of new snowfall by an empirical algorithm; initialize snow layer when the snow accumulation exceeds 10 mm.

Ξ Energy and water balance

Energy balance (thermal.f90)

1) Specific humidity and its derivative at ground surface.
2) Compute sensible and latent fluxes and their derivatives with respect to ground temperature using ground temperatures from previous time step. The iteration calculation of flux-profile is carried in this block.
3) Calculate canopy temperature, latent and sensible fluxes from the canopy, and leaf water storage changed by evaporation. (leaf_tem.f90)

   Leaf temperature
   - Fraction of leaves covered by water.
   - Portion visible canopy absorption (PAR) to sunlit and shaded fractions leaves.

   Iteration:
   - Aerodynamic resistance and bulk boundary layer resistance of leaves; heat conductance for air, leaf and ground.
   - Stomatal resistances for sunlit and shaded fractions of canopy.
   - Leaf temperature based on the energy balance equation.
   - Fluxes: transpiration, evaporation and sensible heat from leaves.
   - Evaluate stability-dependent variables using Monin-Obukhov length for next iteration.
   - The iteration will stop at the convergence criterion of the differences of latent heat from leaves and leaf temperature between two iteration-steps.
     End iteration

   - Derivative of soil energy flux with respect to soil temperature.
   - Update dew accumulation.

4) Ground temperature: thermal conductivity and heat capacity, soil and snow layer temperatures based on the heat conductance equation.
5) Phase changes of water within snow and soil (melt_freezing.f90).
6) Fluxes correction based on the tendency of ground temperature, ground heat flux, outgoing longwave.

Water balance (water.f90)

- Calculation of the water flow within snow and the water masses of liquid and ice portion (wliq and wice) of snow. (water_snow.f90)
- Calculation of the surface runoff and the water infiltration to soil layers.

- Calculation of the water flow within soil and the water mass (wliq) (water_soil.f90)
- Calculation of streamflow and total runoff.
- Root resistance factors and maximum possible transpiration rate.

Ξ Compaction rate for snow; Combine or divide thin or thick snow elements
Ξ Update the snow age

4. Check the water and energy balance (balance_a.f.90)
5. Calendar information for the next time step (ticktime.f90)
6. Ecosystem dynamics: phenology, vegetation, soil carbon or call satellite data to get LAI,.., ect.; Connection node to ecosystem dynamic model. (lai_.f90).
7. Snow fraction cover (fraction of ground covered by snow and fraction of vegetation buried by snow) (fraction_snow.f90)
8. Cosine of solar zenith angle for next-time step (clmzen.f90)
9. Compute albedoes (used in the next step radiation computations) (albedo.f90)
10. Write out the model variables for restart run and output (for off-line run). (restart_save.f90)
11. Return required surface fields to atmospheric model: [kpt] vector of subgrid points $\rightarrow$ [lpt] vector of land points $\rightarrow$ [lon] $\times$ [lat] grid. This mapping is for land points only. Non-land points are undefined. (clm2d_return.f90)

12. $t = t + \Delta t$; return to1***.

Appendix 6: Fortran Symbols

[to be filled after have a fixed code version]

References

Beven, K.J., 1984: Infiltration into a class of vertically non-uniform soils. Hydrol. Sci. J., Vol. 29:505-521.

Campbell, G.S., 1977. An Introduction to Environmental Biophysics. Springer-Verlag, New York.

Clapp B.J. and G.M. Hornberger, 1978: Empirical equations for some soil hydraulic properties. Water Resour. Res., Vol. 14: 601-604.

Collatz, G.J., Ball, J.T., Grivet, C., and Berry, J.A., 1991. Physiological and environmental regulation of stomatal conductance, photosynthesis, and transpiration: a model that includes a laminar boundary layer. Agric. For. Meteorol., Vol. 54: 107-136.

Collatz, G.J., Ribas-Carbo, M., and Berry, J.A., 1992, Coupled photosynthesis-stomatal conductance model for leaves of C_4 plants. Aust. J. Plant Physiol., Vol. 19: 519-538.

Cosby B.J, G.M. Hornberger, R.B. Clapp and T.R. Ginn, 1984: A statistical exploration of the relationships of soil moisture characteristics to the physical properties of soils. Water Resour. Res., Vol. 20: 628-690.

Dai Y. and Q.-C. Zeng 1997: A land surface model (IAP94) for climate studies, Part I: formulation and validation in off-line experiments. Advance Atmospheric Sciences, Vol. 14: 433-460.

Dickinson R.E., A. Henderson-Sellers, P. J. Kennedy, M. F. Wilson, 1993: Biosphere atmosphere transfer scheme (BATS) version 1e as coupled for Community Climate Model. NCAR Tech. Note NCAR/TN-378+STR, 72 pp.

Dickinson, R.E., M. Shaikh, R. Bryant and L. Graumlich, 1998: Interactive Canopies in a Climate Model *J. Climate*, Vol. 11: 2823-2836.

Dougherty, R.L., Bradford, J.A., Coyne, P.I., and Sims, P.L., 1994: Applying an empirical model of stomatal conductance to three C-4 grasses. Agric. For. Meteorol., Vol. 67: 269-290.

Farouki O.T., 1981: Thermal properties of soils. USA Cold Regions Research and Engineering Lab., CRREL Monograph 81-1.

Farquhar, G.D., von Caemmerer, S., and Berry, J.A., 1980: A biochemical model of photosynthetic CO_2 assimilation in leaves of C_3 species. Planta, Vol. 149: 78-90.

Farquhar, G.D., and von Caemmerer, S., 1982: Modeling of photosynthetic response to environmental conditions. pp. 549-587. In: O.L. Lange, P.S. Nobel, C.B. Osmond, and H. Ziegler (eds) Encyclopedia of Plant Physiology. Vol. 12B. Physiological Plant Ecology. II. Water Relations and Carbon Assimilation. Springer-Verlag, New York.

Flatau P.J., R.L. Walko , and W. R. Cottonm, 1992: Polynomial Fits to Saturation Vapor Pressure. J. Appl. Meteor., Vol. 31: 1507-1513.

Fuchs M., G.S. Campbell and R.I. Papendick, 1978: An analysis of sensible and latent heat flow in a partially frozen unsaturated soil. Soil Sci. Soc. of America Journal, Vol. 42(3): 379-385.

Henderson-Sellers B., 1985: New formulation of eddy diffusion thermocline models. Appl. Math. Modeling, Vol. 9: 441-446.

Henderson-Sellers B., 1986: Calculating the surface energy balance for lake a reservoir modeling: a review. Rev. Geophys., Vol. 24: 625-649.

Holtslag, A.A.M., E.I.F. de Bruijn, and H.-L. Pan, 1990: A high-resolution air mass transformation model for short-range weather forecasting. Mon. Wea. Rev., Vol. 118: 1561-1575.

Hostetler S.W. and P. J. Bartlein, 1990: Simulation of lake evaporation with application to modeling lake level variations of Harney-Malheur Lake, Oregon. Water Resource Res., Vol. 26: 2603-2612.

Hostetler S.W., G.T Bates and F. Giorgi, 1993: Interactive coupling of a lake thermal model with a regional climate model. J. Geophys. Res., Vol. 98(D): 5045-5057.

Jordan R., 1991: A one-dimensional temperature model for a snow cover: Technical documentation for SNTHERM.89. USA Cold Regions Research and Engineering Laboratory, Special Report 91-16, 49pp.

Kader, B.A. and A.M. Yaglom, 1990: Mean fields and fluctuation moments in unstably stratified turbulent boundary layers. J. Fluid Mech., Vol. 212: 637-662.

Koster, R.D. and M.J. Suarez, 1992: Modelling the land surface boundary in climate model as a composite of independent vegetation stands; J. Geophys. Res. Vol. 97(D): 2697-2715

Landsberg, J.J., 1986. Physiological Ecology of Forest Production. Academic Press, New Brunswick, New Jersey.

Philip J. R., 1957: Evaporation, and moisture and heat field in the soil. J. Meteorology, Vol. 14: 354-366.

Running, S.W., Loveland, T.R. and L.L. Peerce, 1994: A vegetation classification logic based on remote sensing for using in global scale biogeochemical models, Ambio, Vol. 23: 77-81.

Sellers P.J, D.A. Randall, G.J. Collatz, J.A. Berry, C.B. Field, D.A. Dazlich, C. Zhang, G.D. Collelo and L.B. Bounoua, 1996: A revised land surface parameterization (SiB2) for Atmospheric GCMs, Part I: Model Formulation. J. Climate, Vol. 9: 676-705.

Sellers, P.J., Berry, J.A., Collatz, G.J., Field, C.B., and Hall, F.G., 1992: Canopy reflectance, photosynthesis, and transpiration. III. A reanalysis using improved leaf models and a new canopy integration scheme. Remote Sens. Environ. Vol. 42: 187-216.

Stiegliz M., D. Rind, J. Famiglieti and C. Rosenzweig, 1997: An efficient approach to modeling the topographic control of surface hydrology for regional and global climate modeling. J. Climate, Vol. 10: 118-137.

Yang Z.-L., R.E. Dickinson, A. Robock and K. Ya Vinnikov, 1997: Validation of the snow submodel of the Biosphere-Atmosphere Transfer Scheme with Russian Snow Cover and Meteorological Observation Data. J. Climate, Vol. 10: 353-373.

Yen Y., 1981: Review of thermal properties of snow, ice and sea-ice. CRREL Rep. 81-10.

Zeng, X., and R.E. Dickinson, 1998: Effect of surface sublayer on surface skin temperature and fluxes. J. Climate, Vol.11: 537-550.

Zeng X., M. Zhao and R.E. Dickinson, 1998: Intercomparison of bulk aerodynamic algorithms for the computation of sea surface fluxes using TOGA CORE and TAO data. J. Climate, Vol. 11: 2628-2644.

Zeng X., Y. Dai, R.E. Dickinson and M. Shaikh, 1998: The role of root distribution for climate simulation over land. Geophys. Research Letters, Vol. 25: 4533-4536.